

**Fig. 2.** To assess the effect of edaravone on X-ray-induced apoptosis, mice were treated with edaravone at a final concentration of 0, 3.0, or 6.0 mg/kg BW 30 min prior to X-irradiation. TUNEL staining was performed 48 h after X-irradiation to detect and analyze apoptosis. In the absence of edaravone, there was a significantly higher population of TUNEL-positive cells (A,  $74.9 \pm 3.9$  cells) compared to other groups (B–D). In addition, there was a statistical significance in the difference between the group that received only irradiation and the group that received 3.0 mg/kg edaravone (B and D;  $53.6 \pm 6.1$  cells) ( $*p < 0.05$ ). The difference was more dramatic between the group that was only irradiated and the group that received 6.0 mg/kg edaravone (C and D;  $40.6 \pm 4.0$  cells) ( $**p < 0.01$ ). All micrographs are at 200 $\times$  magnification. Values are presented as mean  $\pm$  SEM. The statistical significance of any difference was determined by analysis of variance (ANOVA). Each bar represents an average of 10 mice.

62.9  $\pm$  2.7%, irradiated without treatment: 60.1  $\pm$  3.8%, irradiated with treatment of 6 mg/kg of edaravone: 61.7  $\pm$  2.5%. In addition, we did not observe a difference in the total amount of time that was spent exploring the 2 objects in the sample and choice phase among all groups (in sample phase, control: 26.0  $\pm$  1.5 s, irradiated without treatment: 24.0  $\pm$  1.7 s, irradiated with 6 mg/kg of edaravone: 20.6  $\pm$  1.4 s, in the choice phase, control: 19.4  $\pm$  1.4 s, irradiated without treatment: 21.0  $\pm$  2.1 s, irradiated with 6 mg/kg of edaravone: 19.2  $\pm$  0.9 s). These results suggested that X-irradiation may not affect non-spatial learning and memory among the 3 groups.

In Morris water maze test, all mice improved their performance when the visible (sessions 1–4) and hidden (sessions

5–10) platforms were used. The irradiated mice that received edaravone treatment (6.0 mg/kg) displayed a significantly better learning performance than the untreated mice after irradiation with 10 Gy in sessions 9 and 10 (at session 9, control: 5.23  $\pm$  0.74 s, 10 Gy-irradiated group: 9.09  $\pm$  1.05 s and 10 Gy-irradiated with edaravone injections (6.0 mg/kg) treatment group: 6.65  $\pm$  1.01 s,  $p = 0.047$ , at session 10, control: 2.06  $\pm$  0.75 s, 10 Gy-irradiated group: 8.99  $\pm$  2.45 s and 10 Gy-irradiated with edaravone injections (6.0 mg/kg) treatment group: 3.75  $\pm$  1.46 s,  $p = 0.032$ ). Data represent means  $\pm$  SD at sessions 9 and 10 (Fig. 4).

It has recently been understood that radiation-induced cognitive dysfunction might be linked to the impairment of hippocampal

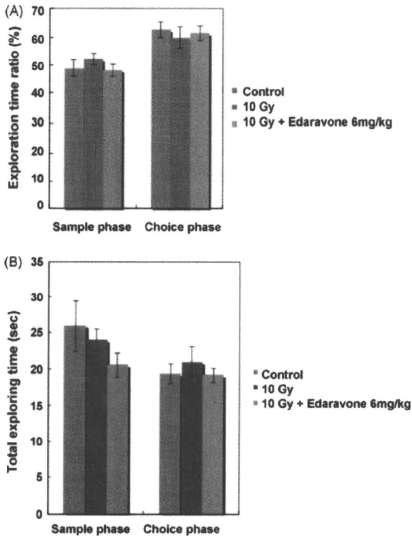


Fig. 3. Novel object recognition test. The exploration time ratio is the time that was spent exploring the new object divided by the total time that was spent exploring the 2 objects. There was no difference in the exploration time ratio and the total amount of time in the sample or choice phase in all groups. Values indicated the means  $\pm$  SEM. Each bar represents an average of 5 mice.

neurogenesis [15,16]. In the hippocampal region of the central nervous system, neurogenesis continues throughout life. The degree of neurogenesis is closely correlated with the hippocampal functions of memory and learning. Neurogenesis in the hippocampus is mediated by the proliferating neural stem or progenitor cells [8]. In patients who received cranial radiation therapy, the altered microenvironment of the stem cells may hinder essen-

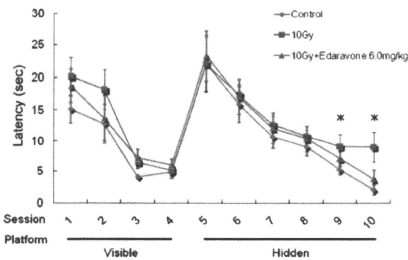


Fig. 4. Water maze performance. Mice were first trained to locate a visible platform (sessions 1–4) and then a submerged hidden platform (sessions 5–10). The time that was needed to reach the platform (latency) was used to quantify the performance. The irradiated mice that received edaravone treatment (6.0 mg/kg) displayed a significantly better learning performance than the untreated mice after irradiation with 10 Gy in sessions 9 and 10 ( $p < 0.05$ ). Each bar represents an average of 5 mice. Points and error bar represent mean and standard deviation (SD), respectively.

tial neurogenesis, thus leading to deficits in learning and memory [14,16].

The present study has extended the results of our previous study by demonstrating that a free-radical scavenger, edaravone, protected human NSCs from radiation-induced cell death. The primary finding of this study in which young mice were used was that neurons in the hippocampus were susceptible to a 10 Gy dose of X-irradiation and that apoptosis was induced. Notably, those apoptotic cells were predominantly observed in the SGZ of the dentate gyrus, presumably among neuronal precursor cells.

Our finding is almost consistent with the fact that neurogenesis in the hippocampus is easily impaired by radiation, although we did not observe apoptosis in the SGZ at 12 h after irradiation, as reported by other studies [13].

Here, we showed that edaravone suppressed X-irradiation-induced apoptosis in neurons in the hippocampus. The clinical therapeutic concentration of edaravone is in concordance with the dose level of 3.0–6.0 mg/kg used in our experiments. These results imply that edaravone can be used as a premedication for cranial radiotherapy. The use of edaravone in premedication should be warranted in a further clinical trial.

Two behavioral tests (i.e., the novel object recognition test and the water maze test) were employed in the present study. The novel object recognition test is based on the natural tendency of mice to investigate a new object instead of a familiar one. The result from this test reflects the learning and recognition memory ability. However, there was no difference in the total amount of time spent on exploring 2 objects in the sample or choice phase in all groups. This test depends on the mood or motivation of the animals, and therefore, it may be difficult to discriminate between control and treated animals. Indeed, few research groups, including even the one which developed this test, reported positive results [6,7]. Unlike the novel object recognition test, the Morris water maze test is widely used to assess the learning and spatial memory in behavioral neuroscience, even though animals are subjected to aversive stimulation to induce a life-threatening escape reaction. This study may indicate the protection of learning and spatial memory in irradiated mice that received edaravone.

In conclusion, we did not address whether edaravone restores neurogenesis in the hippocampus and cognitive function after chronic post-radiation injury. Although further experiments that use animal brain tumor models are required to prove the therapeutic effects, the present study may shed some light on the beneficial effects of free-radical scavengers in impaired neurogenesis following cranial radiotherapy.

#### Acknowledgments

The authors thank Dr. K. Wakai (Department of Preventive Medicine, Nagoya University) for assisting in the statistical analyses. We also thank Dr. A. Nitta (Department of Neuropsychopharmacology, Nagoya University) for giving us suggestions on behavioral pharmacology.

#### References

- V.A. Anderson, T. Godber, E. Smibert, S. Weiskop, H. Ekert, Cognitive and academic outcome following cranial irradiation and chemotherapy in children: a longitudinal study, *Br. J. Cancer* 82 (2000) 255–262.
- A. Boveris, Biochemistry of free radicals: from electrons to tissues, *Medicina (B Aires)* 58 (1998) 350–356.
- C.D. Clelland, M. Choi, C. Romberg, G.D. Clemenson Jr., A. Fragniere, P. Iyers, S. Jessberger, L.M. Saksdia, R.A. Barker, F.H. Gage, T.J. Bussey, A functional role for adult hippocampal neurogenesis in spatial pattern separation, *Science* 325 (2009) 210–213.
- J.R. Crossen, D. Garwood, E. Glarstein, E.A. Newelw, Neurobehavioral sequelae of cranial irradiation in adults: a review of radiation-induced encephalopathy, *J. Clin. Oncol.* 12 (1994) 627–642.

- [5] T.L. Dormandy, Free-radical reaction in biological systems, *Ann. R. Coll. Surg. Engl.* 62 (1980) 188–194.
- [6] A. Ennaceur, J. Delacour, A new one-trial test for neurobiological studies of memory in rats. 1. Behavioral data, *Behav. Brain Res.* 31 (1988) 47–59.
- [7] A. Ennaceur, N. Neave, J.P. Aggleton, Neurotoxic lesions of the perirhinal cortex do not mimic the behavioural effects of fornix transection in the rat, *Behav. Brain Res.* 80 (1996) 9–25.
- [8] F.H. Gage, G. Kempermann, T.D. Palmer, D.A. Peterson, J. Ray, Multipotent progenitor cells in the adult dentate gyrus, *J. Neurobiol.* 35 (1998) 249–266.
- [9] B. Halliwell, Role of free radicals in the neurodegenerative diseases: therapeutic implications for antioxidant treatment, *Drugs Aging* 18 (2001) 685–716.
- [10] A.A. Horton, S. Fairhurst, Lipid peroxidation and mechanisms of toxicity, *Crit. Rev. Toxicol.* 18 (1987) 27–79.
- [11] J. Ishii, A. Natsume, T. Wakabayashi, H. Takeuchi, H. Hasegawa, S.U. Kim, J. Yoshida, The free-radical scavenger edaravone restores the differentiation of human neural precursor cells after radiation-induced oxidative stress, *Neurosci. Lett.* 423 (2007) 225–230.
- [12] J.A. Joseph, The putative role of free radicals in the loss of neuronal functioning in senescence, *Integr. Physiol. Behav. Sci.* 27 (1992) 216–227.
- [13] S. Mizumatsu, M.L. Monje, D.R. Morhardt, R. Rola, T.D. Palmer, J.R. Fike, Extreme sensitivity of adult neurogenesis to low doses of X-irradiation, *Cancer Res.* 63 (2003) 4021–4027.
- [14] M.L. Monje, S. Mizumatsu, J.R. Fike, T.D. Palmer, Irradiation induces neural precursor-cell dysfunction, *Nat. Med.* 8 (2002) 955–962.
- [15] M.L. Monje, T. Palmer, Radiation injury and neurogenesis, *Curr. Opin. Neurol.* 16 (2003) 129–134.
- [16] M.L. Monje, H. Toda, T.D. Palmer, Inflammatory blockade restores adult hippocampal neurogenesis, *Science* 302 (2003) 1760–1765.
- [17] R. Morris, Developments of a water-maze procedure for studying spatial learning in the rat, *J. Neurosci. Methods* 11 (1984) 47–60.
- [18] A. Mouri, L.B. Zou, N. Iwata, T.C. Saïdo, D. Wang, M.W. Wang, Y. Noda, T. Nabeshima, Inhibition of neprilysin by thiorphan (i.c.v.) causes an accumulation of amyloid beta and impairment of learning and memory, *Behav. Brain Res.* 168 (2006) 83–91.
- [19] W. Peissner, M. Kocher, H. Treuer, F. Gillardon, Ionizing radiation-induced apoptosis of proliferating stem cells in the dentate gyrus of the adult rat hippocampus, *Brain Res. Mol. Brain Res.* 71 (1999) 61–68.
- [20] H.F. Poon, V. Calabrese, M. Calvani, D.A. Butterfield, Proteomics analyses of specific protein oxidation and protein expression in aged rat brain and its modulation by L-acetylcarnitine: insights into the mechanisms of action of this proposed therapeutic agent for CNS disorders associated with oxidative stress, *Antioxid. Redox Signal.* 8 (2006) 381–394.
- [21] P.A. Riley, Free radicals in biology: oxidative stress and the effects of ionizing radiation, *Int. J. Radiat. Biol.* 65 (1994) 27–33.
- [22] H. Yoshida, A.H. Kwon, M. Kaibori, K. Tsuji, K. Habara, M. Yamada, Y. Kamiyama, M. Nishizawa, S. Ito, T. Okumura, Edaravone prevents iNOS expression by inhibiting its promoter transactivation and mRNA stability in cytokine-stimulated hepatocytes, *Nitric Oxide* 18 (2008) 105–112.
- [23] N. Zhang, M. Komine-Kobayashi, R. Tanaka, M. Liu, Y. Mizuno, T. Urabe, Edaravone reduces early accumulation of oxidative products and sequential inflammatory responses after transient focal ischemia in mice brain, *Stroke* 36 (2005) 2220–2225.

# Retrovirally engineered T-cell-based immunotherapy targeting type III variant epidermal growth factor receptor, a glioma-associated antigen

Masasuke Ohno,<sup>1</sup> Atsushi Natsume,<sup>1,2,4</sup> Ken-ichiro Iwami,<sup>1</sup> Hidetaka Iwamizu,<sup>1</sup> Kana Noritake,<sup>1</sup> Daiki Ito,<sup>1</sup> Yuki Toi,<sup>1</sup> Motokazu Ito,<sup>1,2</sup> Kazuya Motomura,<sup>1</sup> Jun Yoshida,<sup>1</sup> Kazuhiro Yoshikawa<sup>2,3</sup> and Toshihiko Wakabayashi<sup>1</sup>

<sup>1</sup>Department of Neurosurgery; <sup>2</sup>Center for Genetic and Regenerative Medicine, Nagoya University School of Medicine, Nagoya; <sup>3</sup>Center for Cell Therapy, Aichi Medical University, Nagakute, Aichi, Japan

(Received January 7, 2010/Revised August 21, 2010/Accepted August 23, 2010/Accepted manuscript online September 1, 2010/Article first published online September 30, 2010)

The isotype of epidermal growth factor receptor variant III (EGFRvIII) is often identified in glioblastomas. Previously, we created a mouse monoclonal antibody, 3C10 (IgG2b), that specifically recognized EGFRvIII, and a recombinant single-chain variable fragment of 3C10. The aim of the current study was to develop genetically engineered T cells, termed T-bodies, that express a chimeric receptor consisting of the 3C10 single-chain variable fragment coupled to signaling modules such as the CD3zeta ( $\zeta$ ) chain, for the treatment of tumors expressing mutant EGFR. After successful construction of the chimeric 3C10/CD3 $\zeta$  T-cell receptor, its expression on the T-body was observed using western blotting and flow cytometry. The specificity of the T-body for EGFRvIII was evaluated using an interferon-gamma Elispot assay and a standard <sup>51</sup>Cr-release cytotoxicity assay. Furthermore, we demonstrated that the systemically delivered T-body infiltrated the intracranial tumor and significantly delayed tumor growth. These results indicate that the T-body expressing the chimeric 3C10/CD3 $\zeta$  T-cell receptor specifically recognized glioma cells expressing EGFRvIII. In conclusion, T-body-based immunotherapy appears to be a promising approach for the treatment of glioma. (*Cancer Sci* 2010; 101: 2518–2524)

The expression of epidermal growth factor receptor (EGFR) is amplified in approximately 50% of glioblastomas (GBM).<sup>(1)</sup> The binding of a ligand to EGFR leads to receptor dimerization, autophosphorylation and activation of several downstream signaling pathways such as the Ras/Raf/MEK/ERK pathway, the PI3K/Akt pathway and the PLC-gamma ( $\gamma$ )/PKC pathway, resulting in cell proliferation, motility and survival.<sup>(2)</sup> Approximately 40–70% of brain tumors with EGFR amplification express mutant EGFR variant III (EGFRvIII); EGFRvIII has a deletion of exons 2–7 that causes a defect in the extracellular ligand-binding domain and induces constitutive activation in a ligand-independent manner.<sup>(3–6)</sup> Notably, EGFRvIII is characterized by an 801-base pair (bp) in-frame deletion, which results in a unique sequence with a glycine residue at the fusion junction between amino acid residues 5 and 274. Epidermal growth factor receptor variant III is an attractive target antigen for cancer immunotherapy because it is not expressed in normal tissue and is associated with survival, invasion and angiogenesis in cancers.<sup>(4,7)</sup> Previously, we generated the monoclonal antibody (mAb) 3C10 and a recombinant single-chain variable fragment (scFv) antibody (Ab) that specifically recognizes EGFRvIII.<sup>(8–10)</sup> Glioblastomas cannot be treated and result in death despite the extensive application of surgical excision and adjuvant chemo/radiotherapy. Consequently, various promising immunotherapy approaches for the treatment of glioma are being investigated.<sup>(11–14)</sup>

Cytotoxic T lymphocytes (CTL) are capable of effective recognition and destruction of tumor cells, and therefore cellular

immunotherapy has been suggested for treating tumors in humans.<sup>(15)</sup> However, it is difficult to obtain adequate quantities of tumor-specific T cells. In addition, the isolation and *ex vivo* clonal expansion of tumor-specific CTL from patients is a long and cumbersome process. As a result, general application of this approach has been limited.

Many of the limitations associated with cellular immunotherapy can be circumvented by arming polyclonal CTL with tumor-specific chimeric T-cell receptors (TCR), the so-called “T-body” approach.<sup>(16)</sup> Chimeric TCR typically consist of a tumor antigen-specific recognition scFv element derived from a mAb and components of TCR that mediate signal transduction in the CTL.<sup>(17)</sup> The T-body has the potential to recognize specific antigens in a major histocompatibility complex (MHC)-independent manner; the applicability of this approach has been demonstrated both *in vitro* and *in vivo*.<sup>(18)</sup>

In the present study, we generated human T cells that expressed the scFv-CD3zeta ( $\zeta$ ) chimeric antigen receptor (CAR) targeting the EGFRvIII antigen by using retroviral-mediated transduction. The generated T-body was able to secrete IFN- $\gamma$  and lyse GBM cells in an EGFRvIII-dependent manner. Furthermore, systemic injection of the T-body significantly inhibited intracranial tumor growth in mice.

## Materials and Methods

**Cell lines.** Human GBM cell lines U87MG, expressing wild-type EGFR (EGFRwt), and U87-EGFRvIII, stably expressing EGFRvIII, were kindly provided by Dr W. K. Cavenee (Ludwig Institute for Cancer Research, San Diego, CA, USA). The Jurkat T-cell leukemia cell line was provided by Dr Y. Miyata (Department of Hematology, Nagoya University, Nagoya, Japan). All cell lines were maintained in RPMI-1640 medium containing 10% fetal bovine serum (FBS) and penicillin/streptomycin. The U87-EGFRvIII cell line was maintained in RPMI-1640 medium containing 10% FBS and 400  $\mu$ g/mL geneticin.

**Sample collection and RNA extraction.** Tumor specimens for molecular genetic analysis were obtained from 55 patients with malignant gliomas who underwent surgical procedures at Nagoya University Hospital or affiliated hospitals. The molecular genetic analysis performed in the study was approved by the Institutional Ethics Committee of Nagoya University, and all patients who registered for this study provided written informed consent. All tumors were histologically verified according to World Health Organization 2007 guidelines: 31 patients had GBM (grade IV), 10 had grade III gliomas, and 14 had grade II

<sup>4</sup>To whom correspondence should be addressed.  
E-mail: anatumse@med.nagoya-u.ac.jp

**Table 1. Primers used in the present study**

NheI-leader-V <sub>H</sub>	ACTGCTAGCACC GGTCCTACAATGAAATGCA
AccIII-linker-V <sub>H</sub>	GTCATGGCCGCAAGCTTATTAATTCGGAAACACCACCCGGAACCACCCTCTGAGGAGACTGTGAGAGTGGT
AccIII-linker-V <sub>L</sub>	GCATGGCTCCGGAAGTGGTGGTTCACATATGGATGTGTGATGACCGCACTCCACTCACTCA
VspI-V <sub>L</sub>	TTCCATGGCCGCAAGCTTATTAATGGATCCGGCCACCTGATCGCCGCTCTGACCGTTTTATCTCCAGCTGGTCCCTCCACC
VspI-CD8 $\alpha$	GACATTAAGCCAACTCCAT
BamHI-CD8 $\alpha$	TGCATGGATCCAGGAAGTCCAG
BamHI-CD3 $\zeta$	TGCTGGATCCCAAACCTCTGCT
EcoRI-CD3 $\zeta$	GCTGGAATCTGTTAGCGAGG
EGFR-F	CTTCGGGGAGCAGCGATGCGAC
EGFR-R	ACCAATACCTATCCGTTACAC

Underline indicates restriction enzyme sites. EGFR, epidermal growth factor receptor.

gliomas. RNA purification was performed using the standard TRIzol (Invitrogen, Carlsbad, CA, USA) method.

**EGFR expression analysis by RT-PCR.** Epidermal growth factor receptor variant III expression was examined using RT-PCR assays. First-strand complementary DNA (cDNA) was synthesized from the total RNA (1  $\mu$ g) extracted from 55 tumors and 20 normal tissues (Human Total RNA Master Panel II; Takara Bio, Otsu, Japan) by using the Transcriptor First Strand cDNA Synthesis Kit (Roche, Mannheim, Germany). The cDNA was amplified by PCR using primers designed to flank the 801-bp deleted region (exons 2–7) to detect both EGFRwt and EGFRvIII (Table 1). A 1044-bp PCR product was obtained for EGFRwt, compared with a 243-bp product for EGFRvIII.<sup>(19)</sup>

**Construction of the anti-EGFRvIII CAR.** We constructed 3C10-CAR, a CAR specific to EGFRvIII. 3C10-CAR consists of the 3C10 scFv-Ab against EGFRvIII, which is linked to the hinge portion of human CD8 $\alpha$  ( $\alpha$ ) that is fused to the transmembrane and intracellular signaling domains of the CD3 $\zeta$  chain (Fig. 1). The V<sub>H</sub> and V<sub>L</sub> cDNA fragments of 3C10 were subcloned into the plasmid vector pSRIG-neo, and designated as pSRIG-3C10V<sub>H</sub>-V<sub>L</sub><sup>(10,20)</sup>. The leader sequence V<sub>H</sub> and the first half of the linker domains were subcloned by high-fidelity PCR amplification using pSRIG-3C10V<sub>H</sub>-V<sub>L</sub> as a template, a sense primer including the *NheI* enzyme site (*NheI*-leader-V<sub>H</sub> primer; Table 1) and an antisense primer including the *AccIII* site (*AccIII*-linker-V<sub>H</sub> primer; Table 1). Similarly, the latter half of the linker domain and V<sub>L</sub> domain were amplified with an *AccIII*-linker-V<sub>L</sub> sense primer and a *VspI*-V<sub>L</sub> antisense primer. The two fragments were ligated at the *AccIII* site and inserted into the TA cloning site of the pCR2.1TOPO vector (Invitrogen). The cDNA coding for the hinged portion of CD8 $\alpha$  (aa 95–158) was amplified by PCR using CD8 $\alpha$  cDNA (kindly provided by Dr E. Nakauchi, Department of Immunology, University of Tsukuba, Tsukuba, Japan) as a template and *VspI*-CD8 $\alpha$  sense and *BamHI*-CD8 $\alpha$  antisense primers (Table 1). The cDNA coding for the transmembrane and intracellular portions of CD3 $\zeta$  (aa 142–142) was amplified by PCR using CD3 cDNA (kindly provided by Dr Weissman, National Cancer Institute, Bethesda, MD, USA) as a template and *BamHI*-CD3 $\zeta$  sense and *EcoRI*-CD3 $\zeta$  antisense primers (Table 1). These two fragments were ligated at the *BamHI* site and inserted into the pCR2.1TOPO vector. The leader sequence V<sub>H</sub>-linker-V<sub>L</sub> and the CD8 $\alpha$ -CD3 $\zeta$  cDNA

thus obtained were assembled into the pcDNA3.1 vector at three enzyme sites, *NheI*, *VspI* and *EcoRI*. The sequence of the final construct was confirmed bidirectionally by using the *AccIII*-linker-V<sub>L</sub> forward and *EcoRI*-CD3 $\zeta$  reverse primers.

**Construction of the retroviral vector expressing anti-EGFRvIII CAR.** The retroviral vector backbone pMEI-5 neo vector (Takara Bio) was assembled with the 3C10-CAR construct in pcDNA3.1-3C10-CAR. G3T-hi cells were transfected with pMEI-5 neo-3C10-CAR or pMEI-5 neo-green fluorescent protein (GFP) plasmids along with pGP and pE-ampho packaging plasmids by using the Retrovirus Packaging Kit Ampho (Takara Bio). The cell-free viral supernatants obtained were then frozen and stocked at  $-80^{\circ}\text{C}$ .

**Culture and retroviral transduction of primary human T cells and Jurkat cells.** Freshly harvested peripheral blood mononuclear cells (PBMC) from healthy donors were separated over a monolayer of FicolI (1000g for 20 min at 24 $^{\circ}\text{C}$ ). The PBMC were cultured in AIM-V medium (Invitrogen) with 10% (v/v) human serum in the presence of interleukin 2 (IL-2; 50 U/mL) (Shionogi, Osaka, Japan) and anti-CD3 mAb (muromonab-CD3, 100 ng/mL; Janssen Pharmaceutica, Titusville, NJ, USA) for 48 h. The PBMC were harvested, washed once, and resuspended at a density of  $0.5 \times 10^6$  cells/mL in AIM-V supplemented with 10% (v/v) human serum and IL-2. On day 3, the PBMC ( $0.5 \times 10^6$  cells/mL) were harvested.

For transduction, we precoat a non-tissue culture-treated six-well plate with the recombinant fibronectin fragment FN-CH296 (RetroNectin; Takara Bio) at 100  $\mu$ g per well. The cells were transduced with the retroviral vectors using the viral pre-loading method. Briefly, the FN-CH296-coated plates were loaded with the retroviral vector supernatant and incubated for 4 h at 37 $^{\circ}\text{C}$ . The plate was then washed with phosphate-buffered saline (PBS) and stimulated cells were added (2 mL per well). The cells were then incubated overnight at 37 $^{\circ}\text{C}$ . After adding 4 mL of AIM-V, the cells were transferred to a new six-well plate and incubated with IL-2. After an additional 24 h, 100 nM of Pep3 (LEEKGGNYVVDTHC), a 3C10-specific peptide, was added to the cell culture. The cells were then expanded in the presence of 50 U/mL IL-2 every other day for 1 month.

Jurkat cells ( $5 \times 10^6$  per well) were seeded in a 24-well plate that was precoat with FN-CH296 (25  $\mu$ g per well) as described above. After incubation overnight at 37 $^{\circ}\text{C}$ , the

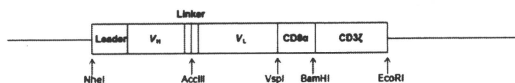


**Fig. 1.** Construction of the anti-epidermal growth factor receptor variant III (EGFRvIII) chimeric antigen receptor. The construct was composed of the V<sub>H</sub> and V<sub>L</sub> regions of the anti-EGFRvIII mAb joined by a flexible linker, a membrane-proximal hinge region of human CD8 $\alpha$ , and the transmembrane and cytoplasmic regions of the human CD3 $\zeta$  chain.

medium was replaced with RPMI-1640 medium containing 10% FBS. Following an incubation period of 72 h, the transduced Jurkat cells were maintained in RPMI-1640 medium containing 10% FBS and 400  $\mu$ g/mL geneticin.

**Western blot analysis.** To confirm the transduction of 3C10-CAR in Jurkat cells, western blot analysis was performed under both nonreducing and reducing conditions. After selection with geneticin, retrovirally transduced Jurkat cells were lysed with cell lysis buffer (Cell Signaling, Danvers, MA, USA), and the lysate was separated by sodium dodecyl sulfate-polyacrylamide gel electrophoresis on 15% resolving gels using standard methods and subsequently blotted onto a polyvinylidene fluoride membrane. The membrane was probed with anti-CD3 $\zeta$  mAb (1:2000; BD Bioscience, Franklin Lakes, NJ, USA) and a horseradish peroxidase-conjugated goat anti-mouse Ab (1:3000), followed by visualization with enhanced chemiluminescence (GE Healthcare Japan, Osaka, Japan).

**Flow cytometry.** The expression of 3C10-CAR on the cell surface of transduced Jurkat cells was examined using a FACS Calibur equipped with the CellQuest research software (Becton Dickinson, Mountain View, CA, USA). Jurkat cells were stained with biotinylated 3C10-specific Pep3 followed by PE-conjugated streptavidin (R&D Systems, Minneapolis, MN, USA).<sup>(8)</sup> The PBMC were stained with fluorescein isothiocyanate (FITC)-conjugated anti-CD4 and PE-conjugated anti-CD8 antibodies (Beckman Coulter Japan, Tokyo, Japan).

**IFN- $\gamma$  Elispot assays.** Cells producing interferon-gamma (IFN- $\gamma$ ) were quantified by ELISPOT (Mabtech, Nacka Strand, Sweden) according to the manufacturer's instructions. Briefly, the PBMC ( $5.0 \times 10^5$ , in triplicate wells) were cultured with anti-CD3 Ab as a positive control or with U87MG or U87-EGFRvIII glioma cells ( $1.0 \times 10^5$ ) and were incubated at 37°C for 24 h. The number of spots in the plate was counted by two observers.

**Target cell lysis.** The susceptibility of U87MG and U87-EGFRvIII cells to PBMC retrovirally transduced with 3C10-CAR was evaluated using a standard 4-h <sup>51</sup>Cr-release assay at various effector:target (E:T) ratios. The percentage of specific lysis was calculated as follows:

$$\frac{100 \times (\text{experimental release} - \text{spontaneous release})}{(\text{maximum release} - \text{spontaneous release})}$$

A target inhibition assay was performed to confirm specific lysis. The PBMC transduced with 3C10-CAR were pre-incubated with various concentrations (0–25  $\mu$ M) of Pep3 for 1 h. Cytotoxicity was assessed at an E:T ratio of 50:1, as described above.

**Intracranial glioma xenograft.** U87-EGFRvIII cells ( $2.5 \times 10^5$ ) suspended in 5  $\mu$ L PBS were injected stereotactically into 5- to 6-week-old NOD/SCID female mice (SLC, Shizuoka, Japan), as described previously.<sup>(21)</sup> Mice bearing established tumors were randomly assigned to two different experimental groups. Four days after tumor inoculation, human PBMC transduced with 3C10-CAR or non-transduced PBMC ( $4 \times 10^6$  cells) were injected into the tail vein. Survival time was assessed after adoptive transfer of the PBMC. To evaluate tumor size, mice were killed at day 12, and brains were fixed in 10% formalin for 24 h and embedded in paraffin. Serial tissue sections (5  $\mu$ m) were stained with hematoxylin and eosin. In order to determine whether the transferred PBMC infiltrated the tumor, paraffin-embedded coronal sections were immunostained with PE-conjugated anti-human CD8 antibody (Dako, Glostrup, Denmark), and nuclei were counterstained with Hoechst 33342. Two perpendicular diameter measurements were obtained for each tumor with calipers. The tumor volume ( $V$ ) was determined using the equation  $V = 0.5 \times a \times b^2$ , where  $a$  is the major axis and  $b$  is the minor axis. Survival and tumor size of treated and control tumors were analyzed using a one-tailed Mann-Whitney test.

## Results

**Determination of EGFRvIII expression.** Epidermal growth factor receptor variant III expression was analyzed in 55 gliomas using RT-PCR. Figure 2A is a representative gel showing the EGFRwt and EGFRvIII PCR products from five gliomas and the U87MG and U87-EGFRvIII cell lines. Epidermal growth factor receptor variant III expression was observed in nine of the 55 tumors. The expression frequency of EGFRvIII in gliomas of grades II, III and IV was 7.1%, 0% and 25.8%, respectively (Fig. 2B). This finding of a higher expression frequency in GBM (grade IV) is consistent with previous studies in which EGFRvIII was identified in approximately 17–57% of GBM.<sup>(5,6,8,22–24)</sup> In addition, all 20 of the normal tissues tested were found to express EGFRwt but not EGFRvIII (Fig. 2C).

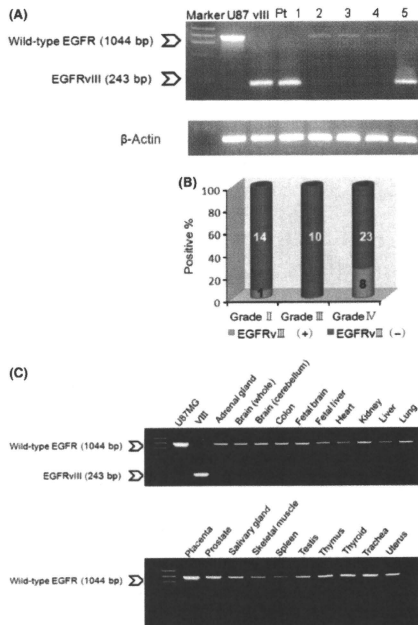


**Fig. 2.** Epidermal growth factor receptor variant III (EGFRvIII) expression in glioblastoma and normal tissues. (A) The detection of EGFRvIII expression in fresh-frozen glioblastoma specimens by RT-PCR. Primers flanking the deleted portion (exons 2–7) amplified cDNA fragments from both full-length EGFR (1044 bp) and the truncated EGFRvIII (243 bp). U87MG (lane 1) and U87-EGFRvIII (lane 2) were included as controls. A representative gel of the PCR products of tumor samples from five patients (Pt.) is shown. Patients (Pt.) 1, 3, 4 and 5 had grade IV tumors, while patient 2 had a grade III tumor. (B) mRNA from 55 glioma samples was isolated and analyzed. The expression frequency of EGFRvIII in grade II, grade III and grade IV tumors was 7.1%, 0% and 25.8%, respectively. (C) EGFR expression in 20 normal tissues. All normal tissues expressed wild-type EGFR but not EGFRvIII.

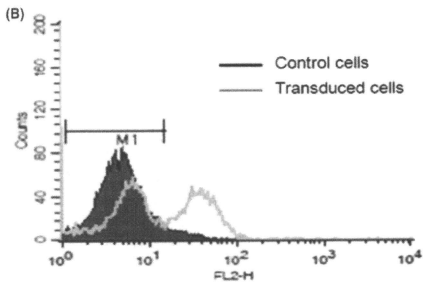
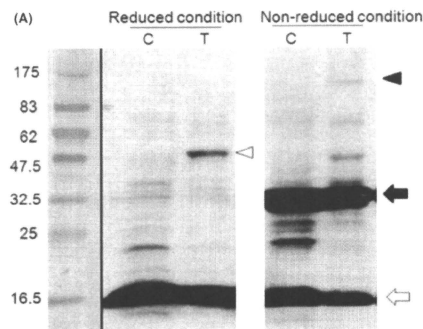


**Fig. 3.** The anti-epidermal growth factor receptor variant III (EGFRvIII)-CD3<sub>3</sub> chimeric antigen receptor (CAR) expression, cell surface trafficking and 3C10 binding on the surface of Jurkat cells. (A) Detection of anti-EGFRvIII-CD3<sub>3</sub> CAR expression in whole-cell lysate derived from Jurkat cell transfectants by reducing and nonreducing western blotting analysis with a mAb specific for the human CD3<sub>3</sub> chain. The lower band (16 kDa) is the endogenous CD3<sub>3</sub> chain (white arrow), and the upper band (32 kDa) is its homodimer (black arrow). The anti-EGFRvIII-CD3<sub>3</sub> CAR was detected at the expected molecular weight of 50 kDa (white arrowhead). The anti-EGFRvIII-CD3<sub>3</sub> CAR homodimer was detected at 100 kDa (black arrowhead). C, control cell; T, transduced cells. (B) Jurkat cells were stained with biotin-conjugated Pep3 and streptavidin-FITC. Expression was not detected in the non-transduced cells (black line). Data are representative of three independent experiments.

**Expression of the anti-EGFRvIII CD3<sub>3</sub> CAR on the surface of Jurkat cells.** The expression of 3C10-CAR was examined by western blot analysis with a mAb specific for the human CD3<sub>3</sub> chain (Fig. 3A). Nonreducing western blot analysis displayed the endogenous monomeric and homodimeric CD3<sub>3</sub> chains at the predicted molecular masses of 16 and 32 kDa, respectively. Reducing western blot analysis showed protein expression corresponding to the predicted mass of the monomeric 3C10-CAR (50 kDa) in transduced cells only; nonreducing western blot analysis detected 3C10-CAR homodimers at a molecular mass of approximately 100 kDa.

To investigate the cell-surface expression of 3C10-CAR, biotin-conjugated Pep3 was used for fluorescence-activating cell sorting analysis. Figure 3B clearly shows the surface expression of 3C10-CAR on transduced Jurkat cells.

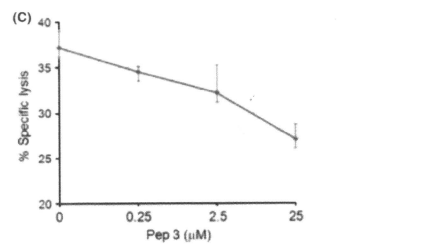
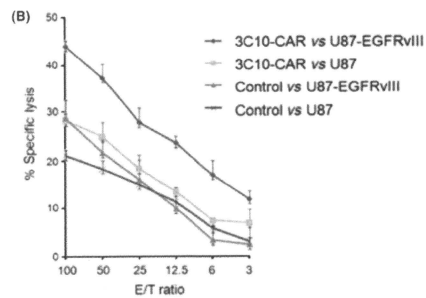
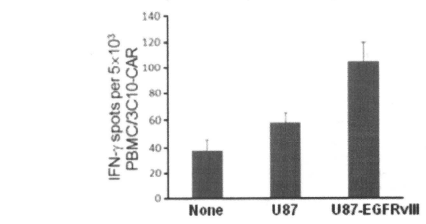
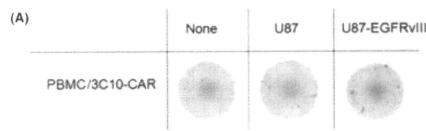


**Fig. 4.** Epidermal growth factor receptor variant III (EGFRvIII)-specific activation of receptor-grafted T cells. (A) Interferon-gamma (IFN- $\gamma$ ) Elispot assay. A 2.5-fold increase in IFN- $\gamma$ -positive spots was observed for 3C10-CAR-transduced PBMC co-cultured with U87-EGFRvIII compared with those co-cultured with U87MG cells. (B)  $^3$ H-T-release assay. 3C10-CAR-transduced PBMC lysed EGFRvIII target cells ( $\bullet$ ) more significantly than other co-cultures. (C) The addition of Pep3 inhibited cytotoxicity. Data are expressed as the mean  $\pm$  standard deviation of three independent experiments.

**Superior IFN- $\gamma$  release and cytotoxicity mediated by 3C10-CAR-transduced T cells.** The IFN- $\gamma$  release and cytotoxicity mediated by 3C10-CAR-transduced PBMC against U87-EGFRvIII and U87MG target cell lines were assessed by Elispot and

$^{51}\text{Cr}$ -release assays. A 2.5-fold increase in IFN- $\gamma$ -positive spots was observed for transduced PBMC co-cultured with U87-EGFRVIII compared with PBMC co-cultured with U87MG cells (Fig. 4A).

To determine whether 3C10-CAR is capable of conferring CTL-mediated lysis against EGFRVIII-positive cells, effector cells were mixed with  $^{51}\text{Cr}$ -labeled target cells. The 3C10-CAR-expressing PBMC exerted significant lysis against U87-EGFRVIII, although some alloreactivity was observed in other effector/target co-cultures (Fig. 4B). The addition of Pep3, which competitively binds to EGFRVIII, inhibited the cytotoxic ability of the 3C10-CAR-expressing PBMC against U87-EGFRVIII in a concentration-dependent manner (Fig. 4C). These observations show that 3C10-CAR-expressing effector cells specifically recognize the EGFRVIII antigen.

**The effect of 3C10-CAR-transduced T cells on EGFRVIII-expressing brain tumor *in vivo*.** Four days after intracranial injections of U87-EGFRVIII cells ( $2.5 \times 10^5$ ), transduced or control PBMC ( $4 \times 10^6$ ) were adoptively transferred via the tail vein. The proportions of CD4+ and CD8+ positive PBMC were 46% and 40%, respectively (Fig. 5A). Although complete tumor

eradication was not observed, tumor growth was significantly retarded in mice injected with 3C10-CAR-transduced PBMC compared with the control ( $P = 0.0472$ ; Fig. 5B). The number of CD8-positive cells that had infiltrated the tumor was greater in mice injected with 3C10-CAR-transduced PBMC than in control mice (Fig. 5C). In addition, the survival time was remarkably prolonged in mice injected with 3C10-CAR-transduced cells (log rank test,  $P = 0.014$ ; Fig. 5D).

## Discussion

**Generation of tumor-specific T cells expressing CAR.** Cellular immunotherapy involving the use of autologous tumor-reactive or host-compatible antigen-specific T cells has significant potential in the treatment of malignant disease.<sup>(25)</sup> However, the degree and persistence of the cellular immunity may be partly limited because of the poor immunogenicity of tumor cells, as evidenced by processes such as MHC silencing. As an alternative strategy, T-bodies have been generated by the transfer of genes encoding CAR. Chimeric antigen receptors consist of a tumor antigen-binding domain of an antibody that has been

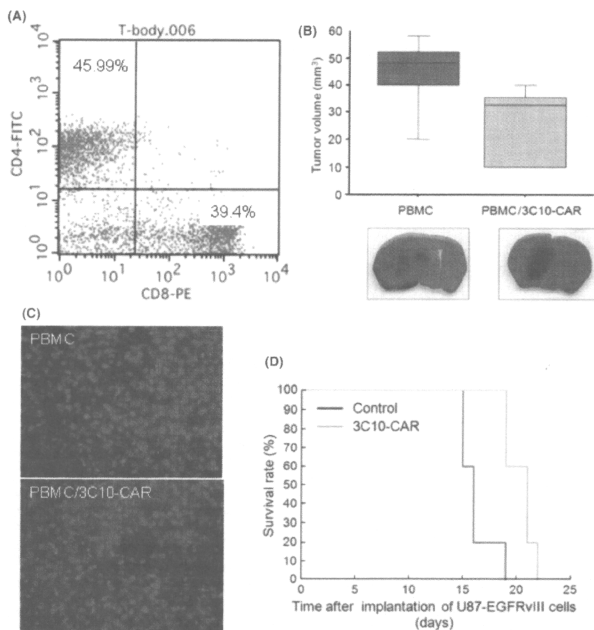


**Fig. 5.** Systemic injection of 3C10-CAR-transduced PBMC retarded the growth of epidermal growth factor receptor variant III (EGFRVIII)-positive tumors in the mouse brain. (A) Among the 3C10-CAR-transduced PBMC, the proportions of CD4+ and CD8+ cells were 45.99% and 39.4%, respectively. (B) At day 12 after tumor inoculation, the tumor volumes were determined; 3C10-CAR-transduced PBMC significantly inhibited tumor growth ( $P = 0.0472$ ). (C) The number of CD8-positive cells that had infiltrated the tumor was greater in mice injected with 3C10-CAR-transduced PBMC than in mice injected with control PBMC. (D) Survival of mice injected with 3C10-CAR-transduced and control PBMC. The survival time of mice injected with 3C10-CAR-transduced PBMC was higher than that of mice injected with control PBMC (log rank test,  $P = 0.014$ ). The number of animals in each group is five.



fused to intracellular signaling domains capable of activating T cells. Therefore, antigen recognition by the T-body is not MHC restricted, and is directed to native cell surface structures. Eshhar *et al.*<sup>16</sup> were the first to create a CAR containing a hapten-specific scFv and the CD3 $\zeta$  chain or Fc $\epsilon$ R1 $\gamma$  chain as the intracellular domain. Several CAR directed against a variety of tumor antigens have been developed. Most of these CAR were transduced in primary mouse and human T cells.<sup>16</sup> In addition, several clinical trials of T-bodies as therapy for ovarian cancer, renal cancer, lymphoma and neuroblastoma are being carried out.<sup>126-31</sup>

**EGFRVIII as a potential target in gliomas.** There are a few fundamental reports relating to the use of T-bodies for tumors of the central nervous system. T cells expressing a CAR consisting of a HER2-specific scFv and domains of the CD3 $\zeta$  chain or CTL expressing IL13-zetakine, which is composed of an extracellular domain that contains the high-affinity IL-13 mutein and a cytoplasmic tail that contains a domain of the CD3 $\zeta$ , have been shown to exert an antitumor effect against experimental medulloblastoma and glioma.<sup>132-34</sup> It is important that target antigens chosen for clinical studies are limited to those expressed only by malignant cells and not by normal cells. A clinical study using T-bodies in patients with renal carcinoma was terminated for the reason of cholestasis as an on-target effect caused by high expression of the targeted antigen carbonic anhydrase in the biliary epithelium. Evidence shows that T-bodies also injured normal cells expressing target molecules, resulting in unfavorable autoimmunity.<sup>127</sup>

The tumor-specific antigens derived from tumor-associated mutations in somatic genes are less likely to be associated with autoimmunity because they are absent in normal tissues. Epidermal growth factor receptor variant III is a rare example of a frequent and consistent tumor-specific mutation that is central to the neoplastic process.<sup>2,3</sup> In this study, the observed frequency of EGFRVIII expression in GBM was 26% (8/31), and this value is relatively lower than the frequency of 17-57% reported in previous studies;<sup>15,6,8,22-24</sup> this finding can be partly attributed to the fact that the number of secondary GBM, in which EGFRVIII expression is less frequent, was large in this study. In addition, we found no EGFRVIII expression in the 10 grade III tumors, but the reason for this could be the small sample size. Nevertheless, the advantages of EGFRVIII include frequent expression in GBM, lack of expression in normal tissues and its importance in the oncogenic phenotype of tumors; these characteristics make EGFRVIII a potential target for antitumor immunotherapy.<sup>8,22,35,36</sup> Therefore, an anti-EGFRVIII CAR has potential as a therapeutic tool.

## References

- Ekstrand AJ, James CD, Cavenee WK, Seliger B, Pettersson RF, Collins VP. Genes for epidermal growth factor receptor, transforming growth factor alpha, and epidermal growth factor and their expression in human gliomas *in vivo*. *Cancer Res* 1991; **51**: 2164-72.
- Zandi R, Larsen AB, Andersen P, Stockhausen MT, Poulsen HS. Mechanisms for oncogenic activation of the epidermal growth factor receptor. *Cell Signal* 2007; **19**: 2013-23.
- Nicholas MK, Lukas RV, Jafri NF, Faoro L, Salsgia R. Epidermal growth factor receptor-mediated signal transduction in the development and therapy of gliomas. *Clin Cancer Res* 2006; **12**: 7261-70.
- Sugawa N, Ekstrand AJ, James CD, Collins VP. Identical splicing of aberrant epidermal growth factor receptor transcripts from amplified rearranged genes in human glioblastomas. *Proc Natl Acad Sci USA* 1990; **87**: 8602-6.
- Frederick L, Wang XY, Eley G, James CD. Diversity and frequency of epidermal growth factor receptor mutations in human glioblastomas. *Cancer Res* 2000; **60**: 1383-7.
- Aldape KD, Ballman K, Furth A *et al.* Immunohistochemical detection of EGFRVIII in high malignancy grade astrocytomas and evaluation of prognostic significance. *J Neuropathol Exp Neurol* 2004; **63**: 700-7.

**Future perspectives.** Recent studies have focused on generating a more effective T-body by improving CAR design. The *in vivo* activation of T-bodies is an important part of this process. CD28, a T-cell costimulatory factor, has been shown to induce T-cell activation and proliferation *in vivo*.<sup>37</sup> Chimeric antigen receptors with dual CD28-CD3 $\zeta$  signaling receptors may enable T cells to proliferate after repeated antigenic stimulation.<sup>38-40</sup> Other costimulatory signaling domains, including 4-1BB, OX40, DAP10 and ICOS, have been investigated.<sup>41-45</sup> In addition, transduction efficiency of the vector should be improved. Intracellular IFN- $\gamma$  assay demonstrated that a proportion of CD8 $^{+}$ /IFN- $\gamma$  cells in CAR-transduced PBMC co-cultured with U87EGFRVIII was 3-7% (data not shown). In order to improve transduction efficiency, lentiviral-mediated transduction might be an alternate approach.

Another potent strategy involves the combination of the EGFRVIII T-body with a kinase inhibitor of the receptor. Epidermal growth factor receptor variant III leads to constitutive activation of downstream signaling pathways, including second messenger pathways.<sup>2,3</sup> Several clinical trials of erlotinib have been conducted in patients with glioma,<sup>44-46</sup> and erlotinib has been found to be effective in a subset of patients whose tumors showed expression of EGFRVIII and phosphatase and tensin homolog deleted from chromosome 10 (PTEN), or high expression of EGFR and low phosphorylation of Akt.<sup>19,46,47</sup> Combined treatment with an anti-EGFRVIII T-body and a tyrosine kinase inhibitor, which targets extracellular and intracellular domains of the receptor, may augment the potency of EGFR signaling inhibition.

In conclusion, we constructed an EGFRVIII-targeted CAR and confirmed its successful retrovirus-mediated expression. We demonstrated the activation and cytotoxicity of genetically engineered T cells both *in vitro* and *in vivo*. Further clinical trials should be conducted to determine the efficacy of T-bodies in the treatment of EGFRVIII-expressing gliomas.

## Acknowledgments

This work was supported by a Grant-in-Aid (B) (A.N.) and a Grant-in-Aid for Young Scientists (B) (M.I.) for Scientific Research from the Ministry of Health, Labor and Welfare, Japan.

## Disclosure Statement

We declare there are no competing financial interests in relation to this work.

- Yamazaki H, Ohba Y, Tamaoki N, Shibuya M. A deletion mutation within the ligand binding domain is responsible for activation of epidermal growth factor receptor gene in human brain tumors. *Jpn J Cancer Res* 1990; **81**: 773-9.
- Humphrey PA, Wong AJ, Vogelstein B *et al.* Anti-synthetic peptide antibody reacting at the fusion junction of deletion-mutant epidermal growth factor receptors in human glioblastoma. *Proc Natl Acad Sci USA* 1990; **87**: 4207-11.
- Okamoto S, Yoshikawa K, Ohata Y *et al.* Monoclonal antibody against the fusion junction of a deletion-mutant epidermal growth factor receptor. *Br J Cancer* 1996; **73**: 1366-72.
- Nakayashiki N, Yoshikawa K, Nakamura K *et al.* Production of a single-chain variable fragment antibody recognizing type III mutant epidermal growth factor receptor. *Jpn J Cancer Res* 2000; **91**: 1035-43.
- Okada H, Kohanbash G, Zhu X *et al.* Immunotherapeutic approaches for glioma. *Crit Rev Immunol* 2009; **29**: 1-42.
- Izumioto S, Tsuboi A, Oka Y *et al.* Phase II clinical trial of Wilms tumor 1 peptide vaccination for patients with recurrent glioblastoma multiforme. *J Neurosurg* 2008; **108**: 963-71.
- De Vleeschouwer S, Fieuws S, Rutkowski S *et al.* Postoperative adjuvant dendritic cell-based immunotherapy in patients with relapsed glioblastoma multiforme. *Clin Cancer Res* 2008; **14**: 3098-104.

- 14 Wheeler CJ, Black KL, Liu G *et al*. Vaccination elicits correlated immune and clinical responses in glioblastoma multiforme patients. *Cancer Res* 2008; **68**: 5955–64.
- 15 Rosenberg SA. Cancer vaccines based on the identification of genes encoding cancer regression antigens. *Immunol Today* 1997; **18**: 175–82.
- 16 Eshhar Z, Waks T, Gross G, Schindler DG. Specific activation and targeting of cytotoxic lymphocytes through chimeric single chains consisting of antibody-binding domains and the gamma or zeta subunits of the immunoglobulin and T-cell receptors. *Proc Natl Acad Sci USA* 1993; **90**: 720–4.
- 17 Sadelain M, Riviere I, Brentjens R. Targeting tumours with genetically enhanced T lymphocytes. *Nat Rev Cancer* 2003; **3**: 35–45.
- 18 Sadelain M, Brentjens R, Riviere I. The promise and potential pitfalls of chimeric antigen receptors. *Curr Opin Immunol* 2009; **21**: 215–23.
- 19 Mellinghoff IK, Wang MY, Vivanco I *et al*. Molecular determinants of the response of glioblastomas to EGFR kinase inhibitors. *N Engl J Med* 2005; **253**: 2012–24.
- 20 Akamizu T, Matsuda F, Okuda J *et al*. Molecular analysis of stimulatory anti-troponin receptor antibodies (TSAbs) involved in Graves' disease. Isolation and reconstruction of antibody genes, and production of monoclonal TSABs. *J Immunol* 1996; **157**: 3148–52.
- 21 Natsume A, Wakabayashi T, Tsujimura K *et al*. The DNA demethylating agent 5-aza-2'-deoxycytidine activates NY-ESO-1 antigenicity in orthotopic human glioma. *Int J Cancer* 2008; **122**: 2542–55.
- 22 Moscatello DK, Holgado-Madruga M, Godwin AK *et al*. Frequent expression of a mutant epidermal growth factor receptor in multiple human tumors. *Cancer Res* 1995; **55**: 5536–9.
- 23 Veloski CE, Ballman KV, Furth AF *et al*. Epidermal growth factor receptor variant III status defines clinically distinct subtypes of glioblastoma. *J Clin Oncol* 2007; **25**: 2288–94.
- 24 Wikstrand CJ, McLendon RE, Friedman AH, Bigner DD. Cell surface localization and density of the tumor-associated variant of the epidermal growth factor receptor, EGFRvIII. *Cancer Res* 1997; **57**: 4130–40.
- 25 Yee C, Thompson JA, Byrd D *et al*. Adoptive T cell therapy using antigen-specific CD8+ T cell clones for the treatment of patients with metastatic melanoma: in vivo persistence, migration, and antitumor effect of transferred T cells. *Proc Natl Acad Sci USA* 2002; **99**: 16168–73.
- 26 Kershaw MH, Westwood JA, Parker LL *et al*. A phase I study on adoptive immunotherapy using gene-modified T cells for ovarian cancer. *Clin Cancer Res* 2006; **12**: 6106–15.
- 27 Lamers CH, Sleijfer S, Vulto AG *et al*. Treatment of metastatic renal cell carcinoma with autologous T-lymphocytes genetically retargeted against carbonic anhydrase IX: first clinical experience. *J Clin Oncol* 2006; **24**: e20–2.
- 28 Lamers CH, Langeveld SC, Groot-van Ruijven CM, Debets R, Sleijfer S, Gratama JW. Gene-modified T cells for adoptive immunotherapy of renal cell cancer maintain transgene-specific immune functions in vivo. *Cancer Immunol Immunother* 2007; **56**: 1875–83.
- 29 Till BG, Jensen MC, Wang J *et al*. Adoptive immunotherapy for indolent non-Hodgkin lymphoma and mantle cell lymphoma using genetically modified autologous CD20-specific T cells. *Blood* 2008; **112**: 2261–71.
- 30 Pale MA, Savoldo B, Myers GD *et al*. Virus-specific T cells engineered to coexpress tumor-specific receptors: persistence and antitumor activity in individuals with neuroblastoma. *Nat Med* 2008; **14**: 1264–70.
- 31 Park JR, Digusto DL, Slovak M *et al*. Adoptive transfer of chimeric antigen receptor re-directed cytolytic T lymphocyte clones in patients with neuroblastoma. *Mol Ther* 2007; **15**: 825–33.
- 32 Ahmed N, Ratnayake M, Savoldo B *et al*. Regression of experimental medulloblastoma following transfer of HER2-specific T cells. *Cancer Res* 2007; **67**: 5957–64.
- 33 Kahlton KS, Brown C, Cooper LJ, Raubitschek A, Forman SJ, Jensen MC. Specific recognition and killing of glioblastoma multiforme by interleukin 13-zetakine redirected cytolytic T cells. *Cancer Res* 2004; **64**: 9160–6.
- 34 Stastny MJ, Brown CE, Ruel C, Jensen MC. Medulloblastomas expressing IL13Ralpha2 are targets for IL13-zetakine- cytolytic T cells. *J Pediatr Hematol Oncol* 2007; **29**: 669–77.
- 35 Garcia de Palazoa IE, Adams GP, Sundareshan P *et al*. Expression of mutated epidermal growth factor receptor by non-small cell lung carcinomas. *Cancer Res* 1993; **53**: 3217–20.
- 36 Wikstrand CJ, Hale LP, Batra SK *et al*. Monoclonal antibodies against EGFRvIII are tumor specific and react with breast and lung carcinomas and malignant gliomas. *Cancer Res* 1995; **55**: 3140–8.
- 37 Gong MC, Latouche JB, Krause A, Heston WD, Bander NH, Sadelain M. Cancer patient T cells genetically targeted to prostate-specific membrane antigen specifically lyse prostate cancer cells and release cytokines in response to prostate-specific membrane antigen. *Neoplasia* 1999; **1**: 123–7.
- 38 Haynes NM, Trapani JA, Teng MW *et al*. Single-chain antigen recognition receptors that costimulate potent rejection of established experimental tumors. *Blood* 2002; **100**: 3155–63.
- 39 Hombach A, Wieczarkowicz A, Marquardt T *et al*. Tumor-specific T cell activation by recombinant immunoreceptors: CD3 zeta signaling and CD28 costimulation are simultaneously required for efficient IL-2 secretion and can be integrated into one combined CD28/CD3 zeta signaling receptor molecule. *J Immunol* 2001; **167**: 6123–31.
- 40 Maher J, Brentjens RJ, Gunset G, Riviere I, Sadelain M. Human T-lymphocyte cytotoxicity and proliferation directed by a single chimeric TCRzeta/CD28 receptor. *Nat Biotechnol* 2002; **20**: 70–5.
- 41 Imai C, Mihara K, Andreansky M *et al*. Chimeric receptors with 4-1BB signaling capacity provoke potent cytotoxicity against acute lymphoblastic leukemia. *Leukemia* 2004; **18**: 676–84.
- 42 Marin V, Kakuda H, Dander E *et al*. Enhancement of the anti-leukemic activity of cytokine induced killer cells with an anti-CD19 chimeric receptor delivering a 4-1BB-zeta activating signal. *Exp Hematol* 2007; **35**: 1388–97.
- 43 Finney HM, Akbar AN, Lawson AD. Activation of resting human primary T cells with chimeric receptors: costimulation from CD28, inducible costimulator, CD134, and CD137 in series with signals from the TCR zeta chain. *J Immunol* 2004; **172**: 104–13.
- 44 de Groot JF, Gilbert MR, Aldape K *et al*. Phase II study of carboplatin and erlotinib (Tarceva, OSI-774) in patients with recurrent glioblastoma. *J Neurooncol* 2008; **90**: 89–97.
- 45 Brown PD, Krishnan S, Sarkaria JN *et al*. Phase I/II trial of erlotinib and temozolomide with radiation therapy in the treatment of newly diagnosed glioblastoma multiforme: North Central Cancer Treatment Group Study N0177. *J Clin Oncol* 2008; **26**: 5603–9.
- 46 van den Bent MJ, Brandes AA, Rampling R *et al*. Randomized phase II trial of erlotinib versus temozolomide or carbustine in recurrent glioblastoma: EORTC brain tumor group study 26034. *J Clin Oncol* 2009; **27**: 1268–74.
- 47 Wang MY, Lu KV, Zhu S *et al*. Mammalian target of rapamycin inhibition promotes response to epidermal growth factor receptor kinase inhibitors in PTEN-deficient and PTEN-intact glioblastoma cells. *Cancer Res* 2006; **66**: 7864–9.



ORIGINAL ARTICLE

# Efficient delivery of liposome-mediated MGMT-siRNA reinforces the cytotoxicity of temozolomide in GBM-initiating cells

T Kato<sup>1</sup>, A Natsume<sup>1,2</sup>, H Toda<sup>1</sup>, H Iwamizu<sup>1</sup>, T Sugita<sup>3,4</sup>, R Hachisu<sup>3,4</sup>, R Watanabe<sup>5</sup>, K Yuki<sup>1</sup>, K Motomura<sup>1</sup>, K Bankiewicz<sup>5</sup> and T Wakabayashi<sup>1</sup>

<sup>1</sup>Department of Neurosurgery, Nagoya University School of Medicine, Nagoya, Japan; <sup>2</sup>Center for Genetic and Regenerative Medicine, Nagoya University School of Medicine, Nagoya, Japan; <sup>3</sup>Hokkaido System Science, Hokkaido, Japan, <sup>4</sup>Division of Diagnostic Pathology, Shizuoka Cancer Center Hospital, Shizuoka, Japan and <sup>5</sup>Department of Neurosurgery, University of California at San Francisco, San Francisco, CA, USA

*Glioblastoma multiforme (GBM) is one of the most formidable brain tumors with a mean survival period of approximately 12 months. To date, a combination of radiotherapy and chemotherapy with an oral alkylating agent, temozolomide (TMZ), has been used as first-line therapy for glioma. However, the efficacy of chemotherapy for treating GBM is very limited; this is partly because of the high activity levels of the DNA repair protein O<sup>6</sup>-methylguanine-DNA methyltransferase (MGMT) in tumor cells, which creates a resistant phenotype by blunting the therapeutic effect of alkylating agents. Thus, MGMT may be an important determinant of treatment failure and should be considered as a suitable target for intervention, in an effort to improve the therapeutic*

*efficacy of TMZ. In this study, we showed that small-interfering RNA (siRNA)-based downregulation of MGMT could enhance the chemosensitivity of malignant gliomas against TMZ. Notably, TMZ-resistant glioma-initiating cells with increased DNA repair and drug efflux capabilities could be efficiently transduced with MGMT-siRNA by using a novel liposome, LipoTrust. Accordingly, such transduced glioma-initiating cells could be sensitized to TMZ in both in vitro and in vivo tumor models. Taken together, this study provides an experimental basis for the clinical use of such therapeutic combinations.*

Gene Therapy advance online publication, 3 June 2010; doi:10.1038/gt.2010.88

**Keywords:** glioma; MGMT; siRNA; TMZ

## Introduction

Glioblastoma multiforme (GBM) is the most lethal form of primary glioma, and the median survival time for patients with GBM is less than 12 months, despite the administration of various therapies, including surgical resection, radiotherapy and chemotherapy.<sup>1</sup> A combination of radiotherapy and chemotherapy with an oral alkylating agent, temozolomide (TMZ), has been used as first-line therapy for glioma. However, the efficacy of TMZ for treating GBM is often very limited because of inherent or acquired resistance. The main determinant of the resistance to alkylating agents is O<sup>6</sup>-methylguanine-DNA methyltransferase (MGMT); this enzyme directly and specifically eliminates the cytotoxic alkyl adducts formed at the O<sup>6</sup> position of guanine and (less frequently) at the O<sup>4</sup> position of thymine.<sup>2,3</sup> Thus, the downregulation of MGMT may enhance the chemosensitivity of malignant gliomas to TMZ.

For many years, gliomas, including GBM, were considered to be heterogeneous bulk tumors composed of differentiated and undifferentiated cells with self-renewal and partial differentiation capabilities.<sup>4</sup> Therefore, glioma treatment failure was attributed to certain undifferentiated tumor cells that were responsible for regrowth. Tumors have been reported to harbor small cell populations possessing growth-sustaining and tumorigenesis capacities. These cells, called cancer stem cells or cancer-initiating cells, have been identified in leukemia, multiple myeloma, breast cancer and glioma. In solid tumors, they show many properties of normal stem cells such as self-renewal and multi-potency, and can also initiate tumor formation. Glioma-initiating cells (GICs) also support the cancer stem cell paradigm. They express genes associated with neural stem cells and differentiate into phenotypically diverse populations, including neuronal, astrocytic and oligodendroglial cells.<sup>5</sup> Moreover, GICs have been reported to contribute to radioresistance and chemoresistance through a preferential checkpoint response and the overexpression of DNA repair genes.<sup>6,7</sup> Indeed, we previously showed that compared with established glioma cell lines (for example, T98G), neurosphere-forming GICs expressed higher levels of MGMT, due to which these cells were far more resistant to TMZ.<sup>8</sup> Consequently, efforts to sensitize

Correspondence: Dr A Natsume, Department of Neurosurgery and Center for Genetic and Regenerative Medicine, Nagoya University School of Medicine, 65 Tsurumai-cho, Nagoya 466-8550, Japan.  
E-mail: anatsume@med.nagoya-u.ac.jp  
Received 9 November 2009; revised 24 April 2010; accepted 24 April 2010

cancer stem-like cells to chemotherapy can be directed at inhibiting molecular pathways involved in stem cell regulation. In addition to the increased DNA repair capacity, cancer stem-like cells may contribute to cytotoxic drug resistance through the expression of proteins associated with drug efflux, such as ATP-binding cassette (ABC) transporters. Normal stem cells and small subpopulations of rat and human glioma cells with stem cell-like properties have previously been identified by their ability to expel the fluorescent dye Hoechst 33342, a compound known to be effluxed by ABC transporters.<sup>9–11</sup> Efflux properties, such as those of the ABC transporters, have been suggested to be significant in maintaining neural stem cells in an undifferentiated state, and in protecting them from toxic substances *in vivo*. Thus, it is crucial to develop a new strategy to target GBM stem cells having drug resistance capacity. Liposome-mediated delivery could bypass the ABC transporters and overcome the drug resistance conferred by these transporters.

In this study, we delivered small-interfering RNA (siRNA) for MGMT encapsulated in cationic liposomes. RNAi therapy requires the development of clinically appropriate, safe and effective drug delivery systems. To this end, we used a novel liposome (LipoTrust EX Oligo) as an *in vivo* delivery system; this liposome has recently been described as an efficient *in vivo* delivery system.<sup>12</sup> In this study, we aimed to examine whether siRNA-based downregulation of MGMT could enhance the chemosensitivity of GICs for TMZ, and to provide an experimental basis for the clinical use of such therapeutic combinations.

## Results

### *MGMT-siRNAs suppress MGMT expression in glioma cell lines*

We first elucidated the knockdown effects of three siRNAs for MGMT (types A, B and C). Two MGMT-expressing glioma cells, T98G and U251 nu/nu, were transduced with these siRNAs by using LipoTrust EX Oligo according to the instruction manual. Reverse transcriptase–polymerase chain reaction (RT–PCR) revealed that all three MGMT-siRNA constructs could efficiently downregulate the expression of MGMT (Figure 1a). We thus used mixed siRNA for further *in vitro* and *in vivo* experiments.

### *MGMT-siRNAs enhance the efficacy of TMZ in MGMT-expressing glioma cell lines*

The glioma cells were treated with an MGMT-siRNA and LipoTrust complex before the addition of TMZ, and the viable cell numbers were measured by the WST assay. MGMT-negative U251SP cells were very sensitive to TMZ alone, and showed no additional toxicity with MGMT-siRNA. In contrast, TMZ alone reduced the number of T98G and U251 nu/nu cells by a mere 13 and 35%, respectively, compared with the dimethyl sulfoxide (DMSO) control. MGMT-siRNA alone showed minimal reduction in T98G cell growth. However, MGMT-siRNA in combination with TMZ induced dramatic cytotoxicity in both cell lines (Figure 1b).

### *Efficient RNAi liposome-mediated delivery in GBM-initiating cells*

We established tumor-initiating cell lines, also known as tumor stem cells, from tumor tissues obtained from GBM patients. Tumor stem cells possibly contain many similar properties to normal stem cells, which may confer a long life span, including relative quiescence, resistance to drugs and toxins through the expression of several ABC transporters,<sup>9,14</sup> and an active capacity for DNA repair.<sup>7</sup> First, we investigated whether LipoTrust efficiently delivers siRNA to GICs that are known to express proteins that have a physiological role in the export of drugs. As shown in Figure 2a, almost all the GICs were successfully transfected with FAM-labeled siRNA by LipoTrust. Previous studies have reported that GICs express abundant levels of MGMT, which could help explain their tremendous capacity for DNA repair.<sup>7,8</sup> The results of conventional RT–PCR as well as real-time PCR confirmed that the MGMT-siRNA/LipoTrust complex effectively downregulated MGMT expression in both GIC lines (Figure 2b).

### *MGMT-siRNA enhances the efficacy of TMZ in GBM-initiating cells*

Glioma-initiating cells were resistant to TMZ alone; this result is in agreement with that of a previous study.<sup>8</sup> MGMT-siRNA in combination with TMZ exerted the greatest antitumor effect. It should be noted that the most substantial cytotoxicity was observed in GICs treated with a combination of MGMT-siRNA and TMZ (Figure 2c).

### *Liposome-mediated siRNA delivery in vivo tumors*

One of the limiting factors in the clinical use of siRNA technology is the delivery to target cells *in vivo*. We investigated whether intratumoral administration of siRNA/LipoTrust complex is efficient in delivering siRNA in subcutaneous glial tumors derived from GICs. First, we injected 80 pmol of an FAM-labeled siRNA/LipoTrust complex intratumorally once a day for 5 days. FAM-siRNA was distributed diffusely within the tumor (Figure 3a). Next, the knockdown of MGMT expression was investigated by using an MGMT-siRNA/LipoTrust complex. MGMT was expressed in 99% of the tumor cells administered with control siRNA, compared with only 7% of cells in MGMT-siRNA-administered tumors (Figure 3b).

### *Treatment of subcutaneous tumor models with a combination of MGMT-siRNA and TMZ*

Subcutaneous glial tumors in nude mice were treated with either TMZ alone, MGMT-siRNA alone or a combination of the two. Mice were separated into four groups (five animals each) (control group, TMZ group, siRNA group and TMZ plus siRNA group) when the diameter of the tumors reached 10 mm. The mice were given intratumoral injections of 80 pmol of siRNA complex or phosphate-buffered saline (PBS) followed by intraperitoneal (i.p.) injections of 50 mg kg<sup>-1</sup> TMZ or DMSO once every day from days 1–5. The tumor growth was not affected in mice administered MGMT-siRNA alone. Mice that were administered TMZ alone showed slight tumor reduction, whereas those received the combination of TMZ and siRNA showed a significant

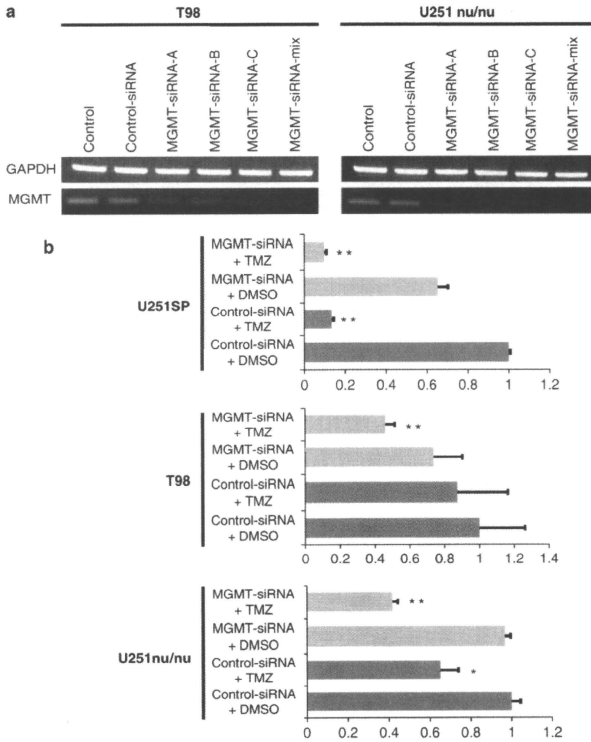


**Figure 1** MGMT suppression by liposome/siRNA complex enhances the efficacy of TMZ in MGMT-expressing glioma cell lines. (a) Two MGMT-expressing glioma cells, T98G and U251 nu/nu, were transfected with three siRNAs for MGMT (types A, B and C) by using LipoTrust. RT-PCR revealed that three MGMT-siRNA constructs could efficiently downregulate the expression of MGMT. (b) The glioma cells were treated with MGMT-siRNA and LipoTrust complex before the addition of TMZ, and the viable cell numbers were measured by the WST assay. MGMT-negative U251SP cells were very sensitive to TMZ alone, and showed no additional toxicity with MGMT-siRNA and TMZ. In contrast, TMZ alone reduced the number of T98G and U251 nu/nu cells by a mere 13 and 35%, respectively, compared with the dimethyl sulfoxide (DMSO) control. MGMT-siRNA alone showed minimal reduction in T98G cell growth, but MGMT-siRNA in combination with TMZ induced dramatic cytotoxicity in both cell lines. \*\* $P < 0.01$ , \* $P < 0.05$  compared with control siRNA+DMSO.

decrease in tumor growth (Figure 4). There was no difference in tumor size between mice that were intratumorally injected with siRNA and control mice that were intratumorally injected with PBS (data not shown).

#### Treatment of brain tumor models in NOD/SCID mice by a continuous drug delivery system

Intracranial inoculation of GICs can generate infiltrative tumors that phenocopy features of parental human GBM tumors, while glioma cell lines tend to form well-demarcated tumors in the brains of mice.<sup>4,5,8</sup> The brain tumor model generated from GICs is ideal to investigate the efficacy of our strategy.

We used an osmotic pump as the drug delivery system, which could supply the siRNA complex at a flow rate of  $0.5 \mu\text{l h}^{-1}$  for a week. We transplanted  $10^5$  cells GICs in the right frontal lobe of NOD-SCID mice, and simultaneously implanted an osmotic pump containing the MGMT-siRNA/LipoTrust complex. TMZ was administered i.p. for 5 consecutive days starting from day 2. Although mice treated with TMZ alone showed longer survival than untreated mice, Kaplan-Meier analysis revealed that mice receiving MGMT-siRNA had a significantly better response to TMZ (Figure 5). This result suggests that inhibiting MGMT expression using MGMT-siRNA sensitizes mice to TMZ treatment in the brain tumor model. This result is similar to that observed in subcutaneous tumor models.

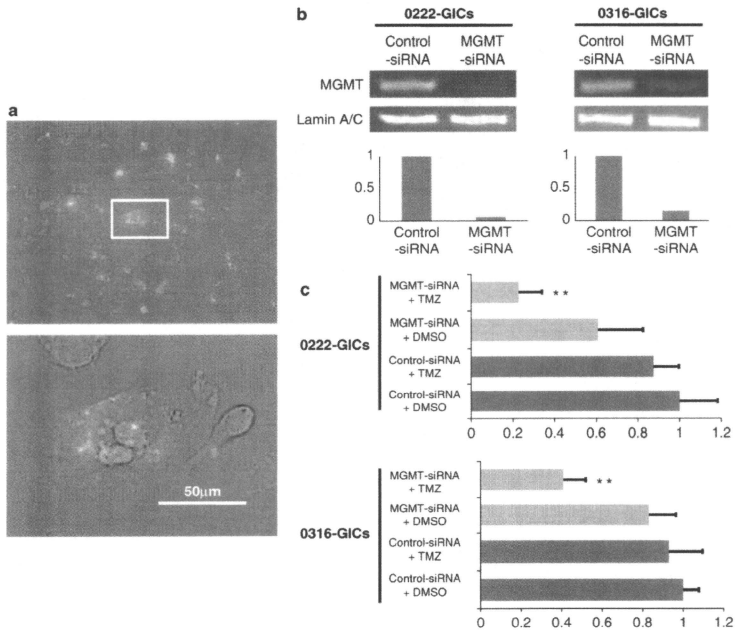


**Figure 2** siRNA for MGMT enhances the efficacy of TMZ in GBM-initiating cells. (a) GBM-initiating cells (GICs) were transfected with FAM-labeled siRNA by LipoTrust. The lower panel shows high magnification of the inset in the upper panel. Almost all the GICs were transfected with FAM-labeled siRNA by LipoTrust. (b) The conventional RT-PCR (upper) as well as real-time PCR (lower) shows that the MGMT-siRNA/LipoTrust complex effectively downregulates the MGMT expression in 0222- and 0316-GIC lines. (c) 0222- and 0316-GICs were treated with MGMT-siRNA and LipoTrust complex before the addition of TMZ, and the viable cell numbers were measured by the WST assay. MGMT-siRNA in combination with TMZ was observed to exert the greatest antitumor effect.  $**P < 0.01$  compared to control-siRNA+DMSO.

## Discussion

The principal finding of this study is that liposome-mediated *in vivo* delivery of MGMT-siRNA efficiently enhanced the cytotoxicity of TMZ in GICs. Notably, although glioma stem cells are considered to have extensive resistance to chemotherapeutic agents due to the high expression of DNA repair-related molecules, our study showed that liposomes were able to deliver the siRNA into glioma stem cells effectively, thus inducing susceptibility to TMZ.

### Overcoming TMZ resistance due to MGMT

MGMT is capable of counteracting the cytotoxicity induced by  $O^6$ -alkylating agents, and the increasing MGMT expression level correlates well with *in vitro* and *in vivo* glioma resistance to TMZ.<sup>15-18</sup> However, in this process, MGMT is rapidly degraded through the ubiquitin/proteasome pathway after receiving alkyl groups from DNA, and the depletion of cellular MGMT pools depends on resynthesis of the molecule.<sup>19</sup> This makes it a

suitable target for intervention in an effort to improve the therapeutic efficacy of TMZ.  $O^6$ -Benzylguanine ( $O^6$ -BG) is a potent inhibitor that irreversibly inactivates MGMT by covalent transfer of its benzyl group to the MGMT active site cysteine residues.<sup>20</sup>  $O^6$ -BG enhances TMZ cytotoxicity in MGMT-proficient glioma cells both *in vitro* and *in vivo*, but not in MGMT-deficient cells.<sup>21</sup> Because patients with MGMT overexpression in the tumors respond more poorly to alkylating agents, co-administration of  $O^6$ -BG to deplete the tumor pools of MGMT to enhance drug cytotoxicity has been previously attempted in clinical settings.<sup>22,23</sup> However, systemic delivery of  $O^6$ -BG increased the myelotoxicity caused by MGMT depletion in bone marrow cells, and therefore the dose of alkylating agents was reduced to a subtherapeutic level. Consequently, none of the patients responded to this drug combination. Therefore, the therapeutic potential of adding  $O^6$ -BG to enhance TMZ cytotoxicity in tumor cells has thus far been discouraging. In this regard, intratumoral delivery of MGMT-siRNA may be more advantageous as compared to  $O^6$ -BG.

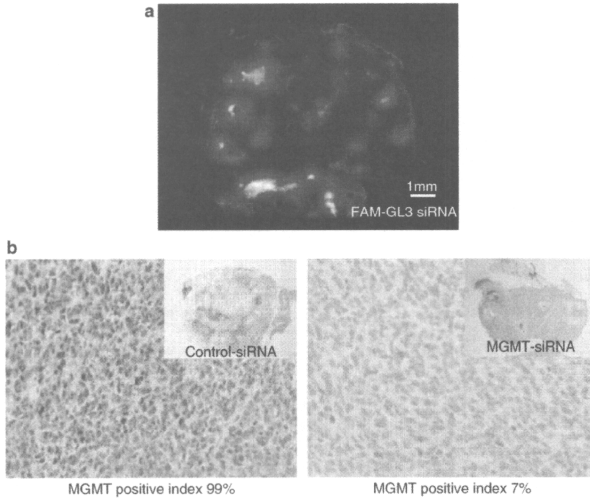


**Figure 3** Liposome-mediated siRNA delivery in *in vivo* tumors. (a) FAM-labeled siRNA/LipoTrust complex (80 pmol siRNA) was injected intratumorally once a day for 5 days. The frozen sections were observed by a fluorescence microscope. FAM-siRNA was distributed diffusely within the tumor. (b) The knockdown by MGMT-siRNA in the subcutaneous tumor was investigated. MGMT was expressed in 99% of the tumor cells injected with control siRNA, whereas MGMT positivity was greatly suppressed to only 7% of MGMT-siRNA-injected tumors.

Use of liposomes to deliver nucleic acids could be an efficient strategy in stem cells that have ABC transporters that render them drug resistant. Unilamellar and multilamellar liposomes are commonly used as pharmaceutical delivery vehicles. In an aqueous environment, one set of polar head groups can form the outer surface of the nanocomplex, whereas another set of polar head groups orients itself to face the interior hydrophilic core, which contains the nucleic acid payload. Liposomes have been used for the delivery of nucleic acids for more than 20 years: Felgner and co-workers<sup>24,25</sup> detailed the ability of the cationic lipid *N*-[1-(2,3-dioleoyloxy)propyl]-*N,N,N*-trimethylammonium chloride to deliver both DNA and RNA into mammalian cell lines. The LipoTrust liposomes used in this study are cationic liposomes suitable for the *in vivo* delivery of siRNAs, antisense DNAs and microRNAs. Recently, Sato *et al.*<sup>26</sup> used vitamin-A-coupled LipoTrust liposomes to deliver anti-gp46 siRNA to fibrogenic hepatic cells for the treatment of liver cirrhosis. LipoTrust was introduced as an *in vivo* siRNA delivery agent in a recent review article.<sup>12</sup> Bypassing the ABC transporters on the cell surface, LipoTrust coupled with MGMT-siRNA can direct intracellular synthesis of the MGMT molecule.

#### Future directions and conclusions

Although liposomes are among the most popular nucleic acid delivery agents, there remain some concerns regarding their safety and delivery efficiency for therapeutic use. The toxicity of certain cationic lipid particles has been reported both *in vitro* and *in vivo*, and certain

synthetic agents have been found to induce a gene signature of their own that might increase the off-target effects of the siRNA. In this study, LipoTrust itself showed *in vitro* cytotoxicity, but no remarkable toxicity was observed *in vivo*. A direct intracerebral approach called convection-enhanced delivery (CED) may be used as a strategy to address these issues.<sup>27–29</sup> CED uses a positive pressure generating a local pressure gradient to distribute agents in the extracellular space. Unlike diffusion delivery, CED is not significantly affected by the concentration, molecular weight or particle size of the agent. Further, CED ensures high concentrations and homogenous distribution of the drug throughout a given target tissue. Further studies should investigate the efficacy of the LipoTrust/MGMT-siRNA complex by the CED in a clinical setting.

## Materials and methods

### Glioma cell lines

The human glioma cell lines U251SP, T98G and U251 nu/nu were obtained from the Memorial Sloan-Kettering Cancer Institute (New York, NY, USA). They were maintained in Dulbecco's modified Eagle's medium (Gibco, Gaithersburg, MD, USA) containing 10% fetal bovine serum, 5 mM L-glutamine, 2 mM nonessential amino acids, and antibiotics (100 U ml<sup>-1</sup> penicillin and 100 µg ml<sup>-1</sup> streptomycin) at 37 °C in a humidified atmosphere with 5% CO<sub>2</sub>. TMZ was supplied by the Schering-Plough Research Institute (Kenilworth, NJ, USA). TMZ was dissolved in DMSO.

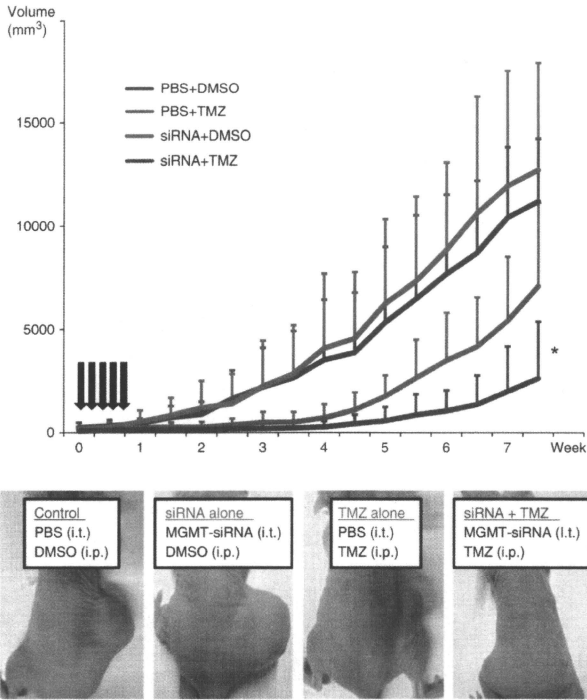


**Figure 4** Treatment of subcutaneous tumor models with a combination of MGMT-siRNA and TMZ. Subcutaneous glioblastoma in nude mice were treated with either TMZ alone, MGMT-siRNA alone or a combination of the two. Mice were separated into four groups (control group, TMZ group, siRNA group and TMZ plus siRNA group) when the diameter of the tumors reached 10 mm. The mice were given intratumoral injections of 80 pmol of siRNA complex or PBS followed by intraperitoneal injections of 50 mg kg<sup>-1</sup> TMZ or DMSO once every day from days 1 to 5. The tumor sizes were then measured using calipers two times every week. Tumor volume was calculated using the following formula: volume (mm<sup>3</sup>) = 0.5236 *d*<sup>3</sup>, where *D* is the longest diameter and *d* the shortest diameter. The tumor growth did not decrease in mice administered MGMT-siRNA alone. Mice that were administered TMZ alone showed slight tumor reduction, whereas the combination of TMZ and siRNA was found to decrease tumor growth significantly. \**P* < 0.05 compared with PBS-DMSO.

#### GBM-initiating cells

Glioblastoma-multiforme-initiating cells were established according to the protocol described previously.<sup>8</sup>

**Tissue collection.** Tumor samples were obtained after consent from the patients (0222 and 0316); the procedure was approved by the Department of Neurosurgery, Nagoya University Hospital, Nagoya, Japan.

**Primary sphere culture.** Tumors were washed and acutely dissociated in PBS (pH 7.4) with 0.1% trypsin (Worthington Biochemical, Freehold, NJ, USA) and 0.04% DNaseI, type II (Sigma-Aldrich, St Louis, MO, USA). The cells were purified using a 70- $\mu$ m cell strainer (BD Falcon, San Jose, CA, USA) followed by

density-gradient centrifugation with Ficoll-Paque Premium (GE Healthcare, Waukesha, WI, USA). The purified cells were then cultured in a 100 × 20 mm Petri dish (BD Falcon) in neurobasal medium (Invitrogen, Carlsbad, CA, USA) containing 2 mM L-glutamine, 0.5% N<sub>2</sub> supplement (Gibco), 1% B27 supplement (Gibco), 20 ng ml<sup>-1</sup> recombinant human epidermal growth factor (rh-EGF; R&D Systems, Minneapolis, MN, USA), and 20 ng ml<sup>-1</sup> rh-basic fibroblast growth factor (bFGF; R&D Systems) in 5% CO<sub>2</sub> at 37 °C.

**Sphere formation.** Approximately 2 weeks later, these cells became spherical, and the spherical cells that had been cultured for at least 2 months were defined as established GICs.



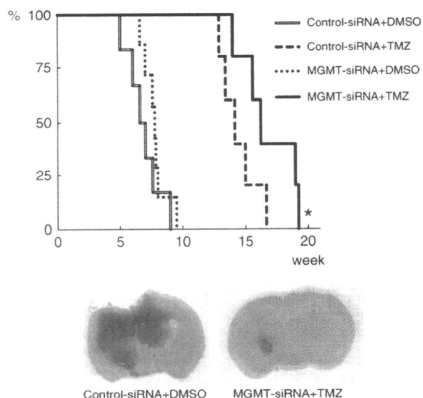


**Figure 5** Treatment of brain tumor models in NOD/SCID mice by continuous drug delivery system. GICs ( $10^5$  cells) in the right frontal lobe of NOD-SCID mice. Simultaneously, an Alzet osmotic pump ( $0.5 \mu\text{l h}^{-1}$  for 1 week) containing 80 pmol siRNA complex was implanted. From day 2, 50 mg  $\text{kg}^{-1}$  of TMZ or DMSO was administered intraperitoneally into the mice for 5 consecutive days. Survival analyses were performed using the Kaplan-Meier method. The mice receiving MGMT-siRNA had significantly better response to TMZ. The representative hematoxylin-eosin-stained brain sections are shown. \* $P < 0.05$  compared with control-siRNA+TMZ.

**Experimental procedure.** One day before the experiments were performed, spherical GICs were dissociated using a NeuroCult chemical dissociation kit (StemCell Technologies, Vancouver, Canada).

#### Preparation of siRNAs

In this study, three siRNA formulations directed against MGMT (B-Bridge, catalog no. SYA21-325, name: 2835KSV\_73, 2835KSV\_284 and 2835KSV\_481) were used. Sense and antisense strands were as follows: MGMT (2835KSV\_73; sequence A) beginning at nt 73: sense, 5'-G AGCAGGGUCUGCAGCAAATT-3' and antisense, 5'-UU UCGUGCAGACCCGUCCTT-3'; MGMT (2835KSV\_284; sequence B) beginning at nt 284: sense, 5'-CCAGACAGG UGUUAUGGAATT-3' and antisense, 5'-LUCCAUAACAC CUGUCUGGTT-3' and MGMT (2835KSV\_481; sequence C) beginning at nt 481: sense, 5'-GGACUGGCCGUGAA GGAAUTT-3' and antisense, 5'-AUUCCUUCACGGCC AGUCCTT-3'. FAM-labeled siRNA against GL3 luciferase, sense 5'-CUUACGCUGAUGACUUCGATT-3'; antisense, 5'-UCGAAGUACUCAGCGUAAAGTT-3'. Negative control siRNA (B-Bridge, catalog no. SSC-0600).

#### Formation of transfection complex

Small-interfering RNAs were transfected into glioma cells by using LipoTrust EX Oligo (Hokkaido System Science, Hokkaido, Japan). A vial of LipoTrust (1  $\mu\text{mol}$  lipid) was reconstituted using 1 ml of nuclease-free water. For *in vitro* experiments, 10  $\mu\text{l}$  of Opti-MEM (Gibco) containing 4 pmol siRNA was gently mixed with

0.5  $\mu\text{l}$  of reconstituted LipoTrust solution (0.4 pmol siRNA/0.05 nmol lipid per  $\mu\text{l}$ ; *in vitro* dose), and incubated for 20 min at room temperature. For animal experiments, 100  $\mu\text{l}$  of Opti-MEM containing 80 pmol siRNA was gently mixed with 8  $\mu\text{l}$  of reconstituted LipoTrust solution (0.8 pmol siRNA/0.08 nmol lipid per  $\mu\text{l}$ ; *in vivo* dose). In a preliminary experiment, an *in vivo* dose of LipoTrust/MGMT-siRNA complex had a knock-down effect on MGMT after incubation for a week at 37 °C (data not shown).

#### Reverse transcriptase-polymerase chain reaction

We plated T98G and U251 nu/nu glioma cells in 100  $\mu\text{l}$  Dulbecco's modified Eagle's medium containing 10% fetal bovine serum at the density of  $1 \times 10^5$  cells per well in a 96-well plate. On day 1, the cells were transfected with the transfection complex described above. Total RNA was extracted from cells by using Trizol reagent (Invitrogen) on day 4. GICs (cultured from patients 0222 and 0316) were plated in 100  $\mu\text{l}$  Dulbecco's modified Eagle's medium containing 10% fetal bovine serum at the density of  $8 \times 10^3$  cells per well in a 96-well plate. Transfection of siRNAs and RNA extraction were performed on days 2 and 5, respectively. Total RNA (500 ng) was subjected to reverse transcription using the Transcriptor First Strand cDNA Synthesis Kit (Roche, Mannheim, Germany). The MGMT forward and reverse primer sequences were 5'-GCAATGAGAGGCAATCCT GT-3' and 5'-CAGTCTCCCGAGTAGTTGC-3', respectively. PCR was performed using GoTaq DNA Polymerase (Promega, Madison, WI, USA) with an initial denaturation step of 94 °C for 5 min; followed by 27 cycles of 94 °C for 30 s, 60 °C for 30 s and 72 °C for 30 s; and a final extension step at 72 °C for 7 min. Glyceraldehyde 3-phosphate dehydrogenase or Lamin A/C PCR products from the same RNA samples were amplified and used as internal controls. cDNA was quantified in a spectrophotometer and diluted to 500 ng  $\mu\text{l}^{-1}$  for use in quantitative real-time PCR. Real-time PCR was carried out using a LightCycler FastStart DNA Master<sup>PLUS</sup> SYBR Green 1 kit (Roche). The PCR reaction was analyzed with a Roche LightCycler. Lamin A/C was used as the internal control.

#### Cell viability assay

The relative cell numbers were determined using a Cell Counting Kit-8 (Dojindo Laboratories, Kumamoto, Japan), a WST-8 cell proliferation assay system, according to the manufacturer's instructions. Glioma cell lines (T98G, U251 SP, and U251 nu/nu cells;  $1 \times 10^3$  cells per well), 0222-GICs and 0316-GICs ( $8 \times 10^3$  cells per well) were added to wells containing Dulbecco's modified Eagle's medium with 10% fetal bovine serum in a 96-well plate. The transfection complex was added to the glioma cell lines on day 1 and to the GIC culture on day 2. After 2 days, 100  $\mu\text{M}$  TMZ or DMSO was added. We then assessed the viability of glioma cell lines 2 days later, and that of GICs, 8 days later.

#### Subcutaneous xenograft tumor model

The 0316-GIC cells ( $1 \times 10^5$  cells) were transplanted subcutaneously in the right flank of BALB/c (nu/nu genotype) nude mice. The tumors were allowed to establish, and they were then passaged *in vivo*. When the subcutaneous tumors had reached a diameter of

10 mm, intratumoral injection of 80 pmol of siRNA/LipoTrust complex (*in vivo* use mixture) and i.p. perfusion of 50 mg kg<sup>-1</sup> of TMZ was performed for 5 consecutive days. PBS administered intratumorally and i.p. perfusion of DMSO were used as the control. The tumor sizes were then measured using calipers two times every week. Tumor volume was calculated using the following formula: volume (mm<sup>3</sup>) = 0.5236 d<sup>2</sup> × D, where D is the longest diameter and d the shortest diameter. The volumes were measured by a single masked observer to prevent observer bias and to avoid inter-operator differences in caliper measurement of the tumors.

**Intracranial xenograft tumor model**

The 0316-GICs (1 × 10<sup>6</sup> cells) were stereotactically injected into the frontal lobe of 6-week-old female NOD-SCID mice. The injection coordinates are as follows: 3 mm to the right of the midline, 2 mm anterior to the coronal suture and 3 mm in depth. Simultaneously, an Alzet osmotic pump (0.5 µl h<sup>-1</sup> for 1 week; 1003D; Durect, Cupertino, CA, USA) containing 80 pmol siRNA complex (for *in vivo* use) was implanted. From day 2, 50 mg kg<sup>-1</sup> of TMZ or DMSO was injected i.p. into the mice for 5 consecutive days. Survival analyses were performed using the Kaplan–Meier method.

**Statistical analyses**

The statistical significance of the observed difference was determined by analysis of variance (StatView software; SAS Institute, Cary, NC, USA), and subsequently, Bonferroni's correction for multiple comparisons was applied. Survival curves were generated using the Kaplan–Meier method. The log-rank statistic (StatView) was used to compare the distribution of the survival times. All reported P-values were two sided; a value less than 0.05 was considered to be statistically significant.

**Conflict of interest**

The authors declare no conflict of interest.

**References**

- 1 Stupp R, Mason WP, van den Bent MJ, Weller M, Fisher B, Taphoorn MJ *et al*. Radiotherapy plus concomitant and adjuvant temozolomide for glioblastoma. *N Engl J Med* 2005; **352**: 987–996.
- 2 Day III RS, Ziolkowski CH, Scudiero DA, Meyer SA, Lubiniecki AS, Girardi AJ *et al*. Defective repair of alkylated DNA by human tumour and SV40-transformed human cell strains. *Nature* 1980; **288**: 724–727.
- 3 Gerson SL. MGMT: its role in cancer aetiology and cancer therapeutics. *Nat Rev Cancer* 2004; **4**: 296–307.
- 4 Lee J, Kotliarova S, Kotliarov Y, Li A, Su Q, Donin NM *et al*. Tumor stem cells derived from glioblastomas cultured in bFGF and EGF more closely mirror the phenotype and genotype of primary tumors than do serum-cultured cell lines. *Cancer Cell* 2006; **9**: 391–403.
- 5 Singh SK, Hawkins C, Clarke ID, Squire JA, Bayani J, Hide T *et al*. Identification of human brain tumour initiating cells. *Nature* 2004; **432**: 396–401.
- 6 Bao S, Wu Q, McLendon RE, Hao Y, Shi Q, Hjelmeland AB *et al*. Glioma stem cells promote reversion by preferential

- activation of the DNA damage response. *Nature* 2006; **444**: 756–760.
- 7 Liu G, Yuan X, Zeng Z, Tunicci P, Ng H, Abdulkadir IR *et al*. Analysis of gene expression and chemoresistance of CD133+ cancer stem cells in glioblastoma. *Mol Cancer* 2006; **5**: 67.
- 8 Yuki K, Natsume A, Yokoyama H, Kondo Y, Ohno M, Kato T *et al*. Induction of oligodendrogenesis in glioblastoma-initiating cells by IFN-mediated activation of STAT3 signaling. *Cancer Lett* 2009; **284**: 71–79.
- 9 Challen GA, Little MH. A side order of stem cells: the SP phenotype. *Stem Cells* 2006; **24**: 3–12.
- 10 Hirschmann-Jax C, Foster AE, Wulf GG, Nuchtern JG, Jax TW, Gobel U *et al*. A distinct 'side population' of cells with high drug efflux capacity in human tumor cells. *Proc Natl Acad Sci USA* 2004; **101**: 14228–14233.
- 11 Patrawala L, Calhoun T, Schneider-Broussard R, Zhou J, Claypool K, Tang DG. Side population is enriched in tumorigenic, stem-like cancer cells, whereas ABCG2+ and ABCG2– cancer cells are similarly tumorigenic. *Cancer Res* 2005; **65**: 6207–6219.
- 12 Whitehead KA, Langer R, Anderson DG. Knocking down barriers: advances in siRNA delivery. *Nat Rev Drug Discov* 2009; **8**: 129–138.
- 13 Dean M, Fojo T, Bates S. Tumour stem cells and drug resistance. *Nat Rev Cancer* 2005; **5**: 275–284.
- 14 Kondo T, Setoguchi T, Taga T. Persistence of a small subpopulation of cancer stem-like cells in the C6 glioma cell line. *Proc Natl Acad Sci USA* 2004; **101**: 781–786.
- 15 Fruehauf JP, Brem H, Brem S, Sloan A, Barger G, Huang W *et al*. *In vitro* drug response and molecular markers associated with drug resistance in malignant gliomas. *Clin Cancer Res* 2006; **12**: 4523–4532.
- 16 Ma J, Murphy M, O'Dwyer PJ, Berman E, Reed K, Gallo JM. Biochemical changes associated with a multidrug-resistant phenotype of a human glioma cell line with temozolomide-acquired resistance. *Biochem Pharmacol* 2002; **63**: 1219–1228.
- 17 Hermisson M, Klumpp A, Wick W, Wischhusen J, Nagel G, Roos W *et al*. O<sup>6</sup>-methylguanine DNA methyltransferase and p53 status predict temozolomide sensitivity in human malignant glioma cells. *J Neurochem* 2006; **96**: 766–776.
- 18 Kokkinakis DM, Bocangel DB, Schold SC, Moschel RC, Pegg AE. Thresholds of O<sup>6</sup>-alkylguanine-DNA alkyltransferase which confer significant resistance to human glial tumor xenografts to treatment with 1,3-bis(2-chloroethyl)-1-nitrosourea or temozolomide. *Clin Cancer Res* 2001; **7**: 421–428.
- 19 Srivenugopal KS, Yuan XH, Friedman HS, Ali-Osman F. Ubiquitination-dependent proteolysis of O<sup>6</sup>-methylguanine-DNA methyltransferase in human and murine tumor cells following inactivation with O<sup>6</sup>-benzylguanine or 1,3-bis(2-chloroethyl)-1-nitrosourea. *Biochemistry* 1996; **35**: 1328–1334.
- 20 Liu L, Gerson SL. Targeted modulation of MGMT: clinical implications. *Clin Cancer Res* 2006; **12**: 328–331.
- 21 Kanzawa T, Bedwell J, Kondo Y, Kondo S, Germano IM. Inhibition of DNA repair for sensitizing resistant glioma cells to temozolomide. *J Neurosurg* 2003; **99**: 1047–1052.
- 22 Quinn JA, Pluda J, Dolan ME, Delaney S, Kaplan R, Rich JN *et al*. Phase II trial of carmustine plus O(6)-benzylguanine for patients with nitrosourea-resistant recurrent or progressive malignant glioma. *J Clin Oncol* 2002; **20**: 2277–2283.
- 23 Quinn JA, Desjardins A, Weingart J, Brem H, Dolan ME, Delaney SM *et al*. Phase I trial of temozolomide plus O<sup>6</sup>-benzylguanine for patients with recurrent or progressive malignant glioma. *J Clin Oncol* 2005; **23**: 7178–7187.
- 24 Malone RW, Felgner PL, Verma IM. Cationic liposome-mediated RNA transfection. *Proc Natl Acad Sci USA* 1989; **86**: 6077–6081.
- 25 Felgner PL, Ringold GM. Cationic liposome-mediated transfection. *Nature* 1989; **337**: 387–388.

- 26 Sato Y, Murase K, Kato J, Kobune M, Sato T, Kawano Y *et al*. Resolution of liver cirrhosis using vitamin A-coupled liposomes to deliver siRNA against a collagen-specific chaperone. *Nat Biotechnol* 2008; **26**: 431–442.
- 27 Bankiewicz KS, Eberling JL, Kohutnicka M, Jagust W, Pivrotto P, Bringas J *et al*. Convection-enhanced delivery of AAV vector in parkinsonian monkeys; *in vivo* detection of gene expression and restoration of dopaminergic function using pro-drug approach. *Exp Neurol* 2000; **164**: 2–14.
- 28 Hadaczek P, Kohutnicka M, Krauze MT, Bringas J, Pivrotto P, Cunningham J *et al*. Convection-enhanced delivery of adeno-associated virus type 2 (AAV2) into the striatum and transport of AAV2 within monkey brain. *Hum Gene Ther* 2006; **17**: 291–302.
- 29 Krauze MT, Vandenberg SR, Yamashita Y, Saito R, Forsayeth J, Noble C *et al*. Safety of real-time convection-enhanced delivery of liposomes to primate brain: a long-term retrospective. *Exp Neurol* 2008; **210**: 638–644.

## Intravenous Methylprednisolone Reduces the Risk of Propofol-Induced Adverse Effects During Wada Testing

Nobuhiro MIKUNI, Youhei YOKOYAMA, Atsuhito MATSUMOTO,  
Takayuki KIKUCHI, Shigeki YAMADA, Nobuo HASHIMOTO\*,  
and Susumu MIYAMOTO

Department of Neurosurgery, Kyoto University Graduate School of Medicine, Kyoto;

\*National Cerebral and Cardiovascular Center, Suita, Osaka

### Abstract

The adverse effects and risks associated with intracarotid propofol injection during Wada testing were retrospectively compared in two groups of patients with ( $n = 75$ ) and without ( $n = 58$ ) intravenous methylprednisolone administered before intracarotid propofol injection. The incidences of all adverse effects were decreased in the methylprednisolone group. In particular, severe adverse effects such as increased muscle tone with twitching and rhythmic movements or tonic posture, which could adversely affect Wada test results, were seen in one patient in the methylprednisolone group and seven patients in the control group, indicating 92% risk reduction. This study suggests that Wada testing using intravenous methylprednisolone administration prior to propofol injection is a safe approach to the preoperative evaluation of brain tumors, epilepsy, and arteriovenous malformations.

Key words: Wada test, methylprednisolone, propofol, adverse effect

### Introduction

The Wada test, a direct intracarotid amobarbital injection that induces transient anesthesia in a single cerebral hemisphere,<sup>11</sup> has been the gold standard for lateralization of hemispheric speech and memory dominance. Although amobarbital has been commonly used for this purpose, its limited availability due to worldwide shortages has led to the exploration of alternative agents such as propofol,<sup>10</sup> methohexital,<sup>2</sup> and etomidate.<sup>6</sup> We have previously reported the clinical utility of an intracarotid propofol test for speech and memory dominance with a moderately high risk of adverse effects.<sup>8</sup> Previous research has suggested that propofol infusion is likely to cause a considerably high incidence of adverse effects, although no data on adverse effects for amobarbital equivalents has been provided.<sup>5</sup>

The present study evaluated the efficacy of methylprednisolone for improving the safety of propofol administration during the Wada test by comparing outcome measures of 75 patients who received methylprednisolone (methylprednisolone group) to those of 58 patients who did not (control

group).

### Patients and Methods

The clinical records were retrospectively examined of all 75 patients (44 men and 31 women), aged 10 to 74 years, who underwent the Wada test from 2006 to 2008 as part of a preoperative examination. The population included 43 patients with brain tumors, 18 patients with temporal or frontal lobe epilepsy, and 14 patients with arteriovenous malformations (AVMs). Fifty-eight patients who underwent the Wada test from 2001 to 2005 using intracarotid propofol without methylprednisolone injection formed the control group in this study. Adverse effects of the control group were reported previously.<sup>8</sup> None of the patients had received steroids before the Wada test.

The methylprednisolone group received an intravenous bolus injection of 500 mg (or 250 mg for children 15 years of age and younger) methylprednisolone at most 5 minutes prior to propofol administration. The Wada test was then performed using the propofol-based protocol reported previously.<sup>8,10</sup> Propofol was administered as a 10 ml saline suspension at a concentration of 1 mg/ml. If this dose did not induce contralateral hemiplegia, addi-

Received December 10, 2009; Accepted February 1, 2010